Volume 1 | Number 1 | Jan 2013 | Pages 1–100

Polymer Chemistry

www.rsc.org/polymers

ROYAL SOCIETY OF CHEMISTRY

ROYAL SOCIETY OF CHEMISTRY

www.rsc.org/polymers

Controlled polymerization of histidine and synthesis of well-defined stimuli responsive polymers. Elucidation of the structure-aggregation relationship of this highly multifunctional material

Dimitrios Mavrogiorgis[1] Panayiotis Bilalis[1], Anastasis Karatzas, Dimitrios Skoulas, Georgia Fotinogiannopoulou, and Hermis Iatrou*

University of Athens, Chemistry Department, Panepistimiopolis, Zografou, 15771, Athens, Greece.

Abstract: We present the synthesis of the novel monomer N^{im}-*trityl*-protected N-carboxy anhydride of L-histidine (*Trt*-HIS-NCA) for the synthesis of poly(L-histidine) (PHIS). Kinetic studies of the ring opening polymerization of *Trt*-HIS-NCA followed first order kinetics indicating that the polymerization is "living". The high purity of the synthesized monomer along with the use of the high vacuum techniques, resulted in the controlled polymerization of histidine in a variety of macromolecular architectures exhibiting high degree of molecular and compositional homogeneity. The conformation of poly(L-histidine) (PHIS) was studied at different pH values and temperatures by Circular Dichroism, revealing that it adopts a random coil conformation at low pH and temperatures, a β-sheet conformation at higher pH, and probably adopts a broken β-sheet conformation at higher temperatures. We found that the pK_a of PHIS homopolymer depends on the molecular weight. Addition of hydrophobic amino acids randomly distributed along the PHIS chain hinders the organization of PHIS, resulting in the formation of random coil conformation even at higher pH. The influence of either leucine (LEU) or *γ-benzyl*-L-glutamate (BLG) randomly distributed along the PHIS chain on the pK_a and degree of protonation in the terpolymers revealed that although pK_a is lower, the protonation of PHIS increases at lower pH values, while it is lower in

---

[1] These authors contributed equally.

a higher pH as compared to that obtained to PHIS. The aggregates of PEO-*b*-P(HIS-*co*-PLEU(BLG)) in water were found to swell more by decreasing the pH and increasing the hydrophobic amino acid, and eventually become disrupted. Surprisingly, at pH=7.4, the increase in temperature leads to lower aggregation of the PEO-*b*-PHIS due to the transition of the secondary structure. The results indicate that it is possible to fine-tune the protonation of PHIS as a function of pH and temperature, and thus control the conditions where the aggregates will be disrupted, a prerequisite for drug and gene delivery applications.

Introduction

Cancer treatment remains a major challenge in medicine, with traditional cancer treatments including surgery, complemented by radiotherapy and/or chemotherapy. Chemotherapy is limited by many constraints, such as severe side effects, nonselective cytotoxicity, prolonged treatment, drug resistance, incomplete cure, and low patient quality of life. In response, pharmaceutical scientists and clinicians are trying to apply nanotechnology to medicine, in order to deliver drugs, genes and proteins with enhanced therapeutic efficacy, reduced dose and low dosing frequency, resulting in fewer side effects. In order to accomplish effective drug and gene delivery to the target site, carriers need to overcome several extra- and intracellular barriers. Poor cancer treatment outcomes result from the nonselective and ineffective delivery of drugs/genes as well as from the development of multidrug resistance (MDR) in tumor cells.[1, 2] In order to address cancer cell treatment issues, novel multifunctional materials are required that will lead to the design and synthesis of "smart" drug delivery systems (DDS).

So far, there are many reports of nanocarriers that successfully accumulate preferably in tumor due to passive and/or active targeting, however their inefficient drug release lowers drug efficacy.[3]

This is due to the lack of vehicles with a triggered release mechanism that do not provide the required quick release of the drug. The rapid drug release could provide the sufficient drug concentration and kill the tumor cells before they acquire MDR. In order to overcome this barrier, vehicles should be developed that will enable the nanocarriers to release drugs in response to specific external or internal stimuli such as pH, temperature, ultrasound, or redox. Among of them, pH-sensitive polymeric vehicles are the most attractive candidates due to intrinsic differences between various solid tumors and the surrounding normal tissues in terms of their relative acidity.[4,5] The microenvironment of solid tumors is quite different from that of normal tissues, the most significant characteristic being the acidic environment that leads to tumor progression, metastatic potential, increased migration, and local invasion, composing a physiological barrier against weak base chemotherapeutic drugs and ultimately induces drug resistance.[4] The measured tumor extracellular pH values of most solid tumors range from pH 6.5 to 6.9 (pHe), while normal blood remains well-buffered and constant at pH 7.4. Moreover, changes in pH are also encountered once a nanocarrier enters cells via endocytosis where pH can drop as low as 5.5-6.5 in endosomes and 4.5-5.5 in lysosomes.[4]

Poly (L-histidine) (PHIS) is a multifunctional material which possesses remarkable properties. The monomeric unit of PHIS has an imidazole ring, and its unsaturated nitrogen has an electron lone pair that can be protonated at pK_a~6.5. This results in a unique property within all natural amino acids, i.e. the amphoteric nature of PHIS within physiological pH range, that renders it soluble at lower pH (~6.3) and insoluble at physiological pH (7.4).[6] Nanocarriers containing PHIS have the ability to control where the drugs will be delivered through its sol-gel pH responsivenes. However, although most pH-sensitive drug carriers are focused on response endosomal pH, most of them release drug outside the tumor cells due to their slightly acidic environment, thus lowering the drug's efficacy.

Nanocarriers featuring ligands complementary to cancer cell surface markers are usually internalized into tumor cells by receptor-mediated endocytosis and entrapped into endosomal/lysosomal vesicles. One of the most difficult barriers that the nonocarrier has to bypass is the disruption of endosome/lysosome vesicles to deliver drugs into the cytosol, especially before they become lysosomes. PHIS has the ability to disrupt the enveloped membrane of endosomes, resulting in early endosomal escape of the PHIS-containing nanocarrier. The PHIS fusogenicity mechanism has been found to proceed through the "proton sponge mechanism".[7-10]

PHIS also reduces chloroauric acid to create Au nanoparticles that present surface plasmon resonance, which can thus be used as "theranostics", that is acting as both therapeutic and diagnostic agents.[11-15] In addition to forming Au nanoparticles, HIS oligomers with six or seven degree of polymerization can be attached on the surface of Au nanoparticles, stabilizing them in an aqueous solution. It has also been found that HIS is the amino acid that appears most frequently in metal binding sites of natural proteins to bind metals such as Cu, Fe, Mn and Zn.[16] HIS also presents very high binding constants with heavy metals such as cobalt and nickel, and has been used in devices and sensors for tracing metals or other species like H_2O_2.[17]

In addition to these properties, PHIS is also capable of condensing DNA through electrostatic interactions between its positive charges and the negative charges of DNA, thus forming polyion complexes. Due to deprotonation of PHIS at higher pH values, condensed DNA is released within physiological pH values.[18] It is obvious that PHIS combines extremely interesting properties related to cancer treatment and can serve as a platform for the synthesis of multifunctional "smart" drug and gene nanocarriers.

In spite of its diverse properties, PHIS presents two drawbacks. Its pK_a~6.5 (depending on the molecular weight can vary slightly), renders it sensitive to the cancer cells' extracellular pHe.[5] The other drawback is its sensitivity to racemization.[19, 20]

Consequently, it is of great importance to synthesize well-defined polymers of this fascinating material with controlled molecular characteristics, low polydispersity featuring the appropriate protecting group that will minimize racemization and that at the same time can be selectively deprotected. In addition, a systematic study is required to elucidate the structure-properties relationship, that will enable scientists to fine-tune the pK$_a$ of PHIS and therefore its aggregation by the experimental conditions such as pH and temperature.

In all synthetic approaches used so far, PHIS- or imidazole-containing polymers were synthesized either by coupling PHIS with another polymer,[7, 10, 21-25] by modifying poly(L-lysine) attaching imidazoles,[8, 9] by the ring opening polymerization (ROP) of the N-carboxy anhydride (NCA) of the protected L-histidine,[26-30] or by repeated liquid phase peptide synthesis.[31] The protecting groups used so far on the ROP of NCA of the protected L-histidine are either benzyl or 2,4-dinitrophenyl groups (DNP). However, the benzyl group can be removed under drastic conditions that can cause rupture of the peptide bond or racemization, while the DNP group cannot be used if disulfide bonds will be utilized for the synthesis of the polymeric materials, since this bond will be ruptured during the deprotection of DNP by thiolysis. To date, even with these protective groups, no work has presented the controlled synthesis of PHIS for the synthesis of well-defined polymers in a variety of different macromolecular architectures with the elucidation of their structure-properties as a function of pH and temperature.

Our group has successfully employed primary amines as initiators along with high vacuum techniques (HVT) to create living conditions for the amino-initiated polymerization of NCAs, a 50-year-old synthetic challenge.[32, 33] With this method, the unwanted activated monomer mechanism is either avoided or is insignificant, thus favoring the desired normal amine mechanism that leads to the synthesis of well-defined polypeptides with complex macromolecular architectures. Our approach is general and we recently showed that it can also be applied to N-substituted amino

5

acids such as L-proline-NCA, where organometallic initiators cannot.[34-38] Since histidine binds very strongly with heavy metals such as nickel and cobalt,[39-42] this property might lead to inability of organometallic initiators to polymerize the NCA of histidine as well. Organometalic initiators are also not able to polymerize sarcosine-NCA, since it is an N-substituted NCA.[38]

Herein, we present the synthesis of the novel monomer N^{im}-trityl protected N-carboxy anhydride of L-histidine (*Trt*-HIS-NCA). The synthetic approach to *Trt*-HIS-NCA was a multi-step procedure, and the purity of the product was very critical since it defined the quality and the ability to control the molecular characteristics (molecular weight and polydispersity) of the PHIS blocks. Kinetics of the polymerization of *Trt*-HIS-NCA confirm that its polymerization rate is approximately 10 times lower than that of the NCA of *γ-benzyl*-L-glutamate. The highly pure *Trt*-HIS-NCA led to the synthesis of homo-, co-, ter- and quarterpolymers with a variety of macromolecular architectures. Well-defined PHIS homopolypetides with molecular weight up to 35 x 10^3 g/mol, the highest ever reported, PEO-*b*-PHIS diblock hybrid copolymers, a series of PEO-*b*-Poly(HIS-*co-γ-benzyl*-L-glutamate(BLG)) with different PHIS/PBLG ratios, a series of PEO-*b*-Poly(HIS-*co*-L-leucine(LEU)) with different PHIS/PLEU ratios, poly(sarcosine)-*b*-PHIS (PSAR-*b*-PHIS) diblock copolypeptides, PEO-*b*-PHIS-*b*-Poly(L-lysine hydrochloride (PLL), PEO-*b*-P(HIS-*co*-BLG)-*b*-PLL, and finally a block-graft PBLG-*b*-(PLL-*g*-P(*Trt*-HIS)) were synthesized. In all polymers, the PHIS block was prepared using the N^{im}-trityl protecting group, which presents the lowest racemization during deprotection and can be deprotected selectively under mild acidic conditions.[43] In all cases the polymers synthesized exhibited very high molecular and compositional homogeneity as revealed by combined characterization results. The influence of the hydrophobic LEU and BLG monomers randomly distributed along the PHIS chain on the pK_a and the degree of protonation as a function of pH was investigated by turbidity measurements and titrations. The pH dependence of the aggregation of PHIS block on the diblock and triblock terpolymers and quarterpolymers was investigated by

dynamic light scattering. It was found that the solubility properties of PHIS are mainly directed by its transition of the secondary structure. For the first time, we report that low molecular weight PHIS is not only pH-responsive, but is also temperature responsive.

Experimental Section

Synthesis of monomers

The synthesis of ε-*tert*-butyloxycarbonyl-L-lysine N-carboxy anhydride (BOCLL-NCA), of γ-benzyl-L-glutamate N-carboxy anhydride (BLG-NCA), of sarcosine N-carboxy anhydride (SAR-NCA) along with of Leucine - N-carboxy anhydride (LEU-NCA) is given in ESI.

Synthesis and characterization of the novel monomer N^{im} -*Trityl* Protected N-Carboxy Anhydride of L-Histidine (*Trt*-HIS-NCA)

The synthesis of *Trt*-HIS-NCA was performed in two steps. In the first step, the HCl salt of *Trt*-HIS-NCA was synthesized, followed by removal of the HCl to afford the pure *Trt*-HIS-NCA monomer.

A. **Synthesis of *Trt*-HIS-NCA.HCl.** In a 500 mL round-bottom flask 20 g (40.2 mmol) of Boc-His(*Trt*)-OH were added and dried overnight under high vacuum. THF (150 ml) (Figure 1a) was distilled in the flask, giving a clear yellowish solution. The reaction flask was placed in an ice-bath, filled with Argon and 3.25 ml (44.2 mmol) of thionyl chloride diluted in 20 ml of THF were added drop-wise over a period of 10 minutes. By the end of addition of thionyl chloride, the solution became yellowish and a small aliquot was analyzed with IR (Figure 1b). Indication that reaction was almost complete was the diminishing of carboxylic acids peak at 1710 cm^{-1} (Figure 1c). After 2 hours the solution was poured in 2 L of cold (Et)$_2$O with precipitation of *Trt*-His-NCA.HCl as the major product (Figure 1d). Finally, the solid was filtered (glass sintered filter 3) and then transferred to a 500 mL round bottom-flask and dried in HV giving 17.2 g. Recrystallization was conducted to the solid mixture, containing the HCl salt, free anhydride and the initial substrate by distilling 300 mL of

7

ethyl acetate under HV. The flask containing the suspension was removed from HV and placed into

a water bath at 45 ^{o}C for 1 hour, resulting in dissolution. The solution was then cooled to 0 ^{o}C with

an ice bath and *Trt*-His NCA.HCl was formed as a precipitate, which was isolated as the only

product after filtration (Figure 1e). The NCA salt was transferred to another flask and dried

overnight under HV (12.5 g=28 mmol). The purity of *Trt*-HIS-NCA.HCl was confirmed by ^{1}H NMR and

IR spectroscopy (^{1}H NMR (300 MHz, CHCl$_{3}$, δ in ppm): 3.20-3.50, (2H, -CH$_{2}$-Imidazole-*Trt*), 4.40-4.60

(1H, N-CH(CH$_{2}$-Imidazole-*Trt*)-C=O of NCA ring), 6.75-7.50 (15H, of trityl group), 8.20-8.30 (1H, N-

CH=C of imidazole ring), 8.65-8.75 (1H,N-CH=N of imidazole ring), IR (thin film): 1848, 1780 cm^{-1}

(vCO, NCA, s), 1620 (n NHCl salt, s), 700cm^{-1}, 748 cm^{-1} (v =C-H out of plane bend, s).

Figure 1

Scheme 1

B. Synthesis of *Trt*-HIS-NCA. Subsequently, 200 ml of EtAc were distilled into the flask, the

flask was removed from HV, filled with Argon and placed in an ice bath. At 0 ^{o}C, 3.5 ml (28 mmol) of

stoichiometric amount of triethylamine dissolved in 50ml of the same solvent were slowly added

drop-wise under vigorous stirring (duration of addition 1 hour). The resulting triethylamine

hydrochloride was filtered off and the filtrate was poured in 1.5 L of non-solvent hexane in order to

recrystallize the *Trt*-His-NCA. A second recrystallization was occurred with a mixture of

solvent/non-solvent EtAc/Hexane (1:5) and the white solid precipitate *Trt*-His-NCA was isolated by

filtration. Finally, *Trt*-HIS-NCA (Figure 1f) was dried under HV overnight and transferred into a glove

box to afford 11.05 g (27 mmol, 67 % yield). The purity of *Trt*-HIS-NCA.HCl was confirmed by ^{1}H

NMR and IR spectroscopy (^{1}H NMR (300 MHz, CHCl$_{3}$, δ in ppm): 2.80-3.20, (2H, -CH$_{2}$-Imidazole-*Trt*),

4.40-4.60 (1H, N-CH(CH$_{2}$-Imidazole-*Trt*)-C=O of NCA ring), 6.75-7.50 (16H, 15 from trityl group and

1 N-CH=C of imidazole ring), 7.60-7.85 (1H,N-CH=N of imidazole ring), IR (thin film): 1848, 1780 cm^{-1}

(vCO, NCA, s), 700 cm^{-1}, 748 cm^{-1} (v =C-H out of plane bend, s). The reactions employed in the synthesis of *Trt*-HIS-NCA are shown in Scheme 1.

Kinetic Studies of HIS-NCA Polymerization. The conditions for the kinetic studies of Trt-HIS-NCA are given in ESI.

Polymer Synthesis

All manipulations were performed under high vacuum in custom-made glass reactors, equipped with break-seals, glass-covered magnets, and constrictions for the addition of reagents and removal of the intermediate products, following well-established high vacuum techniques.[44]

The polymers synthesized are shown in Schemes 2 and 3. Details for the synthesis of the polymers along with the conditions used for Circular Dichroism, Dynamic Light Scattering, turbidity measurements and titrations are given in ESI.

Scheme 2

Scheme 3

Results and Discussion

Synthesis of the NCAs

The synthesis of BLG-NCA, BOCLL-NCA and LEU-NCA has been discussed in our previous works.[32, 45, 46] Their high purity is proved by the ^{1}H NMR and FT-IR analysis (ESI). BOCLL-NCA was utilized because it can be orthogonally deprotected in the presence of PBLG, since it is well established that Boc group can be selectively deprotected with TFA, while benzyl ester group remains intact.

SAR-NCA was synthesized by a route similar to that presented by Fetsch et al.[47] We used high

vacuum to first remove the HCl diadduct of (+)(-) limonene and then to effect the sublimation of

SAR-NCA. The high purity of SAR-NCA synthesized is proved by FT-IR and ^{1}H NMR spectra (Figure F3,

Figure F4 of ESI).

So far, two protecting groups have been used for the synthesis of PHIS, benzyl (Bz) and

dinitrophenyl (DNP) groups. The benzyl group can be deprotected either with Na in liquid ammonia

or HBr in acetic acid, while the DNP group by thiolysis using a thiol. In case of the Bz group, the

conditions are so acidic that almost all protecting groups are deprotected, and therefore, it cannot

be performed selectively if an amphiphilic copolypeptide bearing a protected as well as a free

residue has to be synthesized. The DNP group cannot be used if the molecule contains a disulfide

bond because it will be reduced during thiolysis for the deprotection of DNP.

In addition, many protecting groups of HIS result in racemization during the deprotection

procedure, especially when strong bases are used.[43] The imidazole ring of histidine has two

nitrogens, the π and τ, the first being near and the latter far from the α carbon. Depending on the

protecting group and the conditions of the deprotection, the π nitrogen can abstract the proton of

the α-carbon of the L-isomer resulting to formation of the enol form, and then in the presence of

an acid it can be transformed to the D isomer leading to racemization (Scheme S8, ESI).

In order to avoid racemization, the π nitrogen has to be protected, however this is not possible

for any protecting group. Usually, in order to synthesize a π-protected HIS, first the τ nitrogen is

protected and then is reacted with the appropriate reagent to give the π-protected HIS with

concurrent deprotection of the τ nitrogen. However, this reaction is not quantitative, resulting in a

mixture of HIS with both protecting groups. It is critical to find a protecting group that will be able

to be cleaved selectively under mild conditions and will nor induce racemization. We envisioned

that trityl group fulfills all these requirements. It can be cleaved in the presence of TFA, and,

10

although can only protect the τ nitrogen due to steric hindrance, it is a unique protecting group

that results with the minimum racemization among all protecting groups.[43]

During the synthesis of *Trt*-HIS-NCA, HCl is produced, which is a very strong acid in aprotic

organic solvents, and reacts with the π nitrogen resulting to the corresponding hydrochloride (IR

peak 1620 cm^{-1} in Figure 1d, ^{1}H NMR in Figure 2). We tried to remove the HCl by reacting either

with NaHCO$_3$,[48] however resulted to immediate polymerization of the anhydride due to the

formation of water (NaHCO$_3$ + HCl→NaCl+H$_2$O+CO$_2$). We also used diisopropylethylamine to

remove HCl, however it was not quantitative and in some cases initiation of polymerization

resulted. We found that an equivalent amount of triethylamine resulted in the complete removal

of HCl without any trace of initiation of polymerization. The purity of the monomer was very high

as indicated by the complete lack of any peak at 8.3-8.4 ppm (Figure 3) that would indicate that

either HCl precursor remains in the final product or polymerization has been initiated. The lack of

polymerization is also proved by the absence of any peak at 1650 cm^{-1} in the FT-IR spectrum

characteristic of the peptide bond (Figure 1f). In addition, the lack of any trace of polymerization

proves that the *trityl* group effectively protects both nitrogens, and the slight basicity of the π

nitrogen does not react with the NCA.

Figure 2

Figure 3

Kinetic Studies of the Polymerization of HIS-NCA.

For the "normal amine mechanism" the polymerization rate is given by the following equation:

$$-d[M]/dt=k_p \,[M][I] \Longrightarrow -d\ln[M]/dt=k_{obs} \qquad (1)$$

where the initial slope of the first-order time-conversion plot **k$_{obs}$ = kp[I] (2)** is the observed

rate constant, and **kp** is the rate constant of propagation. In all polymerizations, the molecular

weight increases linearly with the NCA conversion (Figure 4). The polymerization constant

K$_p$=1.9x10^{-4}±0.1 verifies that histidine polymerizes slower than common NCAs of *BOC*-L-lysine and

γ-benzyl glutamate. The half-life times obtained for DP= 20, 50, 100, 200 were t$_{1/2}$= 0.8, 2.3, 4.5 and

9.6 h, respectively. It was found that *Trt*-HIS-NCA polymerizes almost 10 times more slowly than *γ-*

benzyl-L-glutamate.[32] In all monomer to initiator ratios, the *Trt*-His-NCA was completely consumed.

Figure 4

Figure 5

It was found that the polymerization proceeds without termination reactions and follows first

order kinetics, not only as a function of the monomer concentration but also as a function of the

initiator concentration, proving that the polymerization follows the normal amine mechanism. The

linear dependence of the **K$_{obs}$** as a function of initiator concentration (Figure 5) proves the living

nature of the polymerization. Therefore, it is possible to control the molecular characteristics of the

PHIS synthesized from the concentration ratio of [M]/[I], a major requirement for characterizing a

polymerization as "living".

Polymer Synthesis

Initiation by Secondary Amines. Secondary amines react with N-carboxyanhydrides in two

ways, as nucleophiles attacking C(5), thus following the "normal amine mechanism" and the

polymerization is "living" and as bases subtracting the proton on the nitrogen and follow the "activated monomer mechanism" which leads to uncontrolled polymerization.[33] The course of the reaction is dependent on the ratio of nucleophilicity to basicity and on the conditions. Kricheldorf[49] proved by reacting secondary amines with Gly-NCA and N-acetyl-Gly-NCA that secondary amines such as diethylamine acted exclusively as nucleophiles. Bulkier amines like diisopropylamine proceeded with the second route. In other experiments by Kopple[50, 51], various NCAs reacted with secondary and primary amines, almost stoichiometrically. Nucleophiles resulted in amidoamine products which are the initiating species in a polymerization. Dimethylamine (DMA) gave the best results even though it is a secondary amine, indicating that is a very good nucleophile for the polymerization of NCAs. In previous work we incorporated DMA into a plethora of NCAs with excellent results.[35, 37]

PHIS Homopolymers. Efforts to synthesize well-defined PHIS start at 1957, where Patchornik et al.[6] used ring opening polymerization of N^{im}-*benzyl* protected N-carboxy anhydride of L-histidine and either triethylamine or diethylamine as the initiator. They also used triethylamine to remove the HCl from the *Bz*-HIS-NCA.HCl salt initially formed. The polymers synthesized exhibited rather low molecular weight (DP=15) and was treated with sodium in liquid ammonia to remove the protecting benzyl groups. However the only characterization method used was end-group analysis and no data were given for the polydispersity of the polymer.

A few years later, Fridkin et al.[52] synthesized PHIS homopolypeptides by the ring opening polymerization of 2,4-dinitrophenyl group (DNP) N^{im} protected N-carboxy anhydride of L-histidine, initiated by triethylamine. The DNP was removed under very mild conditions by thiolysis. They used the DNP protecting group in order to avoid the removal under drastic procedure such as by treatment of sodium in liquid ammonia which may cause rupture of peptide bonds and

racemization. In this work, the conditions of the deprotection of PHIS were investigated, but no characterization results of the homopolypeptide were given.

More recently, Seong Lee et al.[26] using the 2,4-dinitrophenyl protecting group tried to synthesize PHIS homopolypeptides with various DPs up to 50, as obtained by [1]NMR spectroscopy. However, the highest DP achieved was 33, and no SEC results were presented.

Herein, the reactions used for the synthesis of PHIS homopolymers are shown in Scheme S5 of ESI. We found that the polymerization of *Trt*-HIS-NCA was heterogeneous, i.e. even oligomers of PHIS formed after 6 hours, when the solution turned turbid. The polymerization for the synthesis of the PHIS 6K lasted 6 days, whereas the polymerization of PHIS 35K lasted 9 days. We should point out that it was crucial to completely remove the HCl from the *Trt*-HIS-NCA.HCl salt during the synthesis of the NCA. If traces of the salt remained in the monomer, the addition of dimethylamine resulted in a very slow polymerization rate (more than one month) due to the formation of the HCl salt of the living amine group of the initiator, leading to a lowering of its reactivity.[53] The molecular characteristics of the PHIS homopolypeptides are shown in Table 1. Size exclusion chromatograms of PHIS homopolymers in the system running with a mobile phase TFA/water/acetonitrile are shown in Figure F10, ESI. It is obvious that although the average molecular weight of the higher molecular weight PHIS 35K was that expected from stoichiometry, the polydispersity was higher than that of the lower PHIS 6K, maybe due to the heterogeneity of the polymerization that make the living ends polymerize with lower kinetics due to the lower solubility of the increasing polymeric chain or to retention in SEC columns.

The ^{1}H NMR spectrum of the PHIS 6K was obtained at room temperature using a solution of approximately 1 mL of D_2O with one drop of a 33 % (w/w) DCl solution in D_2O (Figure 6). The lower signal of the peaks of the two protons of the imidazole ring indicate that the protons of the

14

imidazole have different relaxation times and their signal is not comparable with the protons of -

CH$_2$ group or the α proton.

Figure 6

Synthesis of Hybrid Diblock Co-, Terpolymers and Copolypeptides.

Seong-Lee et al in 2003[26] synthesized PEO-*b*-PHIS. The synthetic approach involved the use of

an amino end-functionalized PEO as the macroinitiator for the ROP of DNP-protected HIS-NCA.

They synthesized low molecular weight copolymers, however no characterization results of the

hybrid copolymers were presented.

A few years later, Kim et al.[27] synthesized PEO-*b*-P(HIS-*co*-L-phelylalanine) copolymers by first

modifying α,ω-dihydroxy PEO to α-hydroxyl-ω-carboxyl PEO, followed, after the synthesis of the

amine end-functionalized poly(HIS(N^{im} Bz)-*co*-L-phenylalanine), with the coupling of the carboxyl

group of PEO with the amine group of the copolypeptide. Finally, the low molecular weight diblock

terpolymers were deprotected with sodium in liquid ammonia. Under these conditions

racemization of PHIS may occur, and although the polymers were characterized by SEC, no results

concerning the polydispersity indices were presented.

Johnson et al.[28, 54] synthesized poly(2-hydroxyethyl methacrylate)-*b*-PHIS diblock copolymers.

The synthetic approach involved first the synthesis of the poly(2-hydroxyethyl methacrylate) by

ATRP, transformation of the end-functionalized bromine to amine group, and use this polymer as

the macroinitiator for the silazane-mediated controlled ROP of *Bz*-protected HIS-NCA to result the

diblock copolymer. Finally, the Bz group was cleaved by reacting with HBr/AcOH and TFA at 0 ^{o}C.

The SEC eluograms of the synthesized copolymers showed that there were always some poly(2-

hydroxyethyl methacrylate) homopolymer left unreacted, that was not removed by fractionation.

More recently, the same group synthesized a series of dual stimuli responsive synthetic polymer bioconjugate chimeric materials, comprised of poly(N-isopropylacrylamide)-*b*-poly(L-histidine),[30] with PHIS having degree of polymerization from 50 up to 125. They employed reversible addition–fragmentation chain transfer polymerization of N-isopropylacrylamide, followed by ring–opening polymerization of α-amino acid N-carboxy anhydride of N^{im}-benzyl protected L-histidine. Deprotection of PHIS was performed by treatment of the block copolymer with a 4-fold molar excess of a 33 wt % solution of HBr in acetic acid for 2 h at 0 °C. The dual stimuli responsive properties of the resulting biocompatiable polymers were investigated for their use as a stimuli responsive drug carrier for tumor targeting.

The reactions that we used for the synthesis of PEO-*b*-PHIS, PEO-*b*-P(HIS-*co*-BLG) and PEO-*b*-P(HIS-*co*-LEU) are shown in Schemes 4, 5 and 6, respectively. The name of the polymers containing a block of PHIS with randomly distributed of either BLG or LEU monomers will be indicated as PEO-*b*-P(HIS-*co*-BLG (LEU)-X) where X is 10, 20 and 40, which represents the HIS/BLG (LEU) ratio of 100-X/X.

Scheme 4

Scheme 5

Scheme 6

We found that in the case of the PEO-*b*-PHIS diblock hybrid copolymer, the polymerization became heterogeneous after 12 hours, as indicated by the turbidity, and increased by time. In case of the copolymerizations of *Trt*-HIS-NCA and either BLG-NCA or LEU-NCA, the absolute lack of heterogeneity of the copolymerizations (in contrast to the homopolymerization of PHIS homopolypeptides with exactly the same molecular weight) indicates that the BLG and LEU monomeric units are randomly distributed along the PHIS chain. In addition, this implies that the

heterogeneous polymerization of PHIS is due to the secondary structure probably of α-helix, which does not develop during the copolymerization (probably random coil conformation), as was shown in the study with Circular Dichroism (CD) discussed below. The composition of the blocks of the random copolypeptides of HIS and either LEU or BLG was found to be exactly the same with the feed ratio of NCAs. The molecular characteristics of the synthesized polymers are provided in Table 1. The excellent agreement (within 10 %) between the stoichiometric and the experimentally obtained molecular weights, along with the low polydispersity indices indicate the high degree of molecular and compositional homogeneity of the copolymers. The SEC eluograms of the PEO-*b*-PHIS along with PEO-*b*-P(HIS-*co*-BLG-20) and PEO-*b*-P(HIS-*co*-LEU-20) are shown in Figures F11, F12 and F13 of ESI, respectively. The corresponding ^{1}H NMR spectra are shown in Figures 7, 8 and 9.

Figure 7

Figure 8

Figure 9

Synthesis of the PSAR-*b*-PHIS copolypeptide.

The reactions used for the synthesis of the copolypeptides PSAR-*b*-PHIS 1 and 2 are shown in Scheme 7. Two samples of PSAR-*b*-PHIS copolypeptides were synthesized. The SEC chromatograms of the PSAR precursor along with the final copolypeptide PSAR-*b*-PHIS 1 are provided in Figure F14 of ESI. The molecular characteristics are shown in Table 1. The good agreement of the stoichiometric with the final copolypeptide and the low polydispersity indices of both polymers indicate the high degree of molecular and compositional homogeneity of the final copolypeptide.

17

The [1]NMR spectrum is shown in Figure F8 of ESI. To our knowledge, this is the first diblock

copolypeptide of PSAR with PHIS.

Scheme 7

Synthesis of triblock terpolymer of the type PEO-*b*-PHIS-*b*-PLL along with the triblock

quarterpolymer PEO-*b*-P(HIS-*co*-BLG-15)-*b*-PLL

Liu et al.[55] have synthesized pH-sensitive PEO-*b*-PHIS-*b*-PLLA triblock terpolymers, where PLLA

is poly(L-lactide). The synthetic procedure first involved the synthesis of the PEO-*b*-P(HIS(DNP))

copolymer by using the amino end-functionalized PEO as the macroinitiator of the ROP of DNP-

protected HIS-NCA. PLLA was then synthesized and the terminal hydroxyl group was transformed

to carboxyl group by reaction with succinic anhydride, followed by coupling with the terminal

amine group of the PEO-*b*-P(HIS(DNP)) and deprotection of PHIS with a thiol. The polydispersity

indices of the final terpolymers were as high as 1.87-1.94, revealing incomplete coupling and

presence of the PEO-*b*-PHIS precursors.

Lee et al.**[56]** have synthesized triblock teroplymers of the PLLA-*b*-PEO-*b*-PHIS type. The synthetic

strategy involved the use of a PLLA-*b*-PEO-COOH carboxyl terminated diblock copolymer and

transformation of the carboxyl group to thiol, followed by coupling with an NHS-ester of a carboxyl

terminated PHIS. The molecular weight distribution of the triblock was 1.37, obtained by MALDI-

TOF.

The reactions that we employed in the synthesis of the PEO-*b*-P(HIS-*co*-BLG-15)-*b*-PLL triblock

quarterpolymer are shown in Scheme 8. The SEC chromatogram of the quarterpolymer that we

synthesized along with the corresponding [1]NMR spectrum are shown in Figures F9 of ESI and Figure

10, respectively. The molecular characteristics obtained are shown in Table 1. The good agreement

between the stoichiometric and the final copolypeptides indicate the high degree of molecular and compositional homogeneity. The composition obtained in the block of the final random copolypeptide P(HIS-*co*-BLG) was very close to monomer feed.

Figure 10

Scheme 8

Synthesis of PBLG-*b*-(PLL-*g*-P(*Trt*-HIS)) block-graft terpolypeptide.

Putnam et al.[10] have synthesized PHIS-*g*-PEO graft copolymers. The synthetic approach employed involved the reaction of cyanouril-activated PEO with the τ-nitrogen of the imidazole ring. The purification was performed by dialysis to remove unreacted precursors. Unfortunately no characterization results are given with SEC.

Park et al.[29] have synthesized poly(ethyleneimine)-*g*-(Pethyleneimine-*b*-PHIS-*b*-PEO) graft terpolymers. Their synthetic approach involved the use of an oligoethyleneimine as the macroinitiator for the ROP of Bz-HIS-NCA, followed by the conjugation of a PEO-NHS ester to the amine-end groups of benzyl protected PHIS. The protection was cleaved with treatment of Na in liquid ammonia resulting in the graft terpolymer. No characterization results for the terpolymer were provided in this work.

We utilized a PBLG-*b*-PLL block copolypeptide and the amine groups of PLL as the macroinitiator for the HV ROP of *Trt*-HIS-NCA, resulting in a block-graft terpolypeptide. The procedure utilized for the synthesis of the PBLG-*b*-(PLL-*g*-PHIS) block-graft terpolypeptide is shown in Scheme 9. The SEC eluogram of the initial PBLG block, the copolypeptide PBLG-*b*-PLL and of the final graft is given in Figure 11. The molecular characteristics of the precursors along with the final terpolypeptide are given in Table 1. It is obvious that the final terpolypeptide exhibits very low

polydispersity index and the good agreement between the stoichiometric and the final molecular weights of the blocks indicate the high degree of molecular and compositional homogeneity. This is also supported by the ^{1}H NMR results (Figure 12), which agree with the stoichiometric amounts of the NCAs used. The PLL block has 10 monomeric units, and we maintain that all blocks initiated the polymerization of *Trt*-HIS-NCA. Even though high molecular weight poly(*Trt*-HIS) is not soluble in pure DMF since the homopolymerization of *Trt*-HIS-NCA is heterogeneous, the final terpolypeptide was soluble in the mobile phase of the SEC instrument operating in a 0.1 N LiBr solution of DMF at 60 $^{\circ}$C, due perhaps to the low molecular weight of each grafted poly(*Trt*-HIS) chain. To our knowledge, this is the first block-graft PHIS containing terpolypeptide.

Figure 11

Figure 12

Scheme 9

Dependence of the secondary structure of PHIS on pH and temperature.

Circular Dichroism (CD) of PHIS Homopolymers and PEO-*b*-PHIS Copolymer.

CD measurements were performed on the two PHIS homopolypeptides. The Circular Dichroism (CD) data for the PHIS 6K homopolypeptide at various pH values are provided in Figure F15 in ESI section. In the case of the PEO-*b*-PHIS copolymer, the conformation of the PHIS as a function of pH was almost identical to that of the PHIS 6K homopolypeptide (Figure 13). This is reasonable since the PHIS block is almost identical to the PHIS 6k homopolypeptide. It is obvious that at pH lower than 5, the conformation is mainly random coil. The repulsion among the protonated HIS

monomeric units does not allow the polypeptide to form a 3D structure. However, by increasing the pH, the conformation becomes β-sheet, as indicated by the negative peak at 217 nm, and probably also contains an α-helix conformation, which is indicated from the negative peak at 235 nm (indicated by the arrow). It is obvious that at pH>5.0 the random coil conformation disappears and at the same time a β-sheet conformation starts to develop quickly, as indicated by the rapid lowering of the positive peak at 220 nm obtained at lower pH values and the development of a negative at 217 nm and a positive peak at 188 nm.

The results for the PHIS homopolypeptide along with the PEO-*b*-PHIS copolymers are very similar to those obtained by Myer et al.[57], who also attributed the peaks at higher pH to a mixture of mainly β-sheet and a smaller amount of the α-helix conformation. However, Peggion et al.[58] found that the conformation of PHIS at higher pH values is complicated and cannot be attributed to a simple β-sheet conformation. They also reported that at low pH the charged PHIS exhibits a random coil conformation. In the case of the PHIS homopolymeptide, it was not possible to obtain a spectrum at pH higher than ~6.4 because of precipitation, while in case of the diblock copolymer and diblock terpolymers containing PEO, the polymers remained in solution due to the presence of PEO chains.

The influence of temperature on the conformation of PHIS 6K at pH=7.40 was examined at 3, 10, 20, 37, 50 and 80 °C. Surprisingly, it was found that the conformation was changed from temperatures higher than 37 °C, as depicted in Figure 14. It was found that upon increasing the temperature, the negative peak at 217 nm diminished, while the maximum of the positive peak at 202 nm was shifted to 208 nm, and the negative peak at 188 nm was shifted to 193 nm. This can be assigned to the transformation of the β-sheet conformation of PHIS to a more complicated structure that will be explained below. At low pH values (<4.0) with the random coil conformation, this temperature transition did not take place. When the sample was cooled back from 80 °C to 20

^{o}C, the spectrum was identical to that obtained during heating from 10 at 20 ^{o}C, revealing that for

the PHIS 6K the transition of the conformation as a function of temperature and pH was reversible.

CD measurements were also performed at the PHIS 35K at various pH values at 20 ^{o}C.

Surprisingly, even at the low pH values of 5 and temperature 20 ^{o}C, the conformation obtained was

similar to the one found at 80 ^{o}C at pH=7.40 for the PHIS 6K. The CD spectra are shown in Figure 15.

Increasing the temperature did not have an impact on the conformation of the homopolypeptide

35K.

The PHIS 35K has a rather high molecular weight and the persistence length of PHIS is

significantly lower than this molecular weight. The PHIS segments adopting the *β*-sheet

conformation are lower than 35K and therefore the *β*-sheet conformation is interrupted (broken).

This phenomenon also occurs in the PHIS 6K, but only at higher temperatures. Consequently, the

CD spectrum of PHIS 35K at higher pH values and low temperatures, which is identical to that

obtained at intermediate pH values and high temperatures on the PHIS 6K, can be attributed to a

mixed conformation of broken *β*-sheet segments. For the first time, we observed the temperature

dependence of the low molecular weight PHIS conformation (Scheme 10).

Figure 13

Scheme 10

Figure 14

Figure 15

Circular Dichroism of Diblock Terpolymers.

A thorough study was performed to elucidate the influence of LEU monomeric units randomly distributed along the PHIS on the PEO-*b*-PHIS diblock copolymer along with the PEO-*b*-P(HIS-*co*-LEU-x) terpolymers, where x=10, 20 and 40.

The spectrum for PEO-*b*-P(HIS-*co*-LEU-10) (Figure 16), is completely different from that of PEO-*b*-PHIS. It starts with the random coil conformation in very low pH (pH=3.24-4.79), while at pH=4.79 it starts to develop a *β*-sheet conformation. However, here the random coil conformation does not disappear with the increase of *β*-sheet conformation but rather co-exists with the *β*-sheet over the entire pH range. Poly(L-leucine) adopts an *α*-helix conformation even in oligomers. However, here due to its random distribution along the PHIS chain, cannot become organized to form the *α*-helix conformation and at the same time prevents the PHIS from adopting 100% *β*-sheet conformation, so a small amount of PHIS remains with the random coil conformation even at very high pH values, where practically all PHIS is deprotonated.

Figure 16

When the molar amount of LEU increased to 20 % (Figure 17), the random coil conformation dominated over the entire pH range 3.00-8.22. However, here at an intermediate pH=5.15, a peak is observed at 195 nm together with a peak at 232 nm, indicating the development of an *α*-helical conformation. The peak at 195 nm disappears at higher pH values, while the peak at 232 nm becomes stronger. The data indicate the presence of a random coil conformation which dominates, together with a small amount of the *α*-helical conformation.

Figure 17

In case of the PEO-*b*-P(HIS-*co*-LEU-40), the conformation is a random coil at lower pH where

PHIS is charged, but adopts α-helix conformation gradually, upon increasing the pH, when PHIS

deprotonates. Here, the tendency of PLEU to form α-helices dominates and at higher pH the main

conformation is α-helix as indicated by the negative peak at 226 and the positive peak at 195 nm.

However, at this pH the random coil conformation also remains, corresponding to a small peak at

210 nm indicated by the arrow, probably adopted by the HIS monomers.

The influence of a hydrophobic amino acid randomly distributed along the PHIS chain as a

function of pH was studied for the first time. The tendency of PLEU to form α-helices[59] direct the

P(HIS-*co*-LEU-40) block to adopt this conformation when it is 40 % molar ratio (Figure 18). It was

found that LEU hinders PHIS from forming the β-sheet conformation when it is deprotonated, and

the copolypeptide always contains a small amount of random coil conformation, indicated by the

arrow on Figure 18.

Figure 18

Influence of LEU and BLG on the pK$_a$ and Protonation of PHIS.

Donnini et al.[60] have studied the deprotonation of the imidazole and histidine molecules as a

function of pH. They also obtained the pK$_a$ of either τ or π nitrogens for these two molecules and

found that for the simple imidazole ring, the titration curve was a typical, sharp curve developed

within pH=6-8. The pK$_a$ of the two nitrogens were the same since they are equivalent and equal to

7.28. In the case of histidine, the nitrogens are not equivalent and pK$_a$=6.53 for the π nitrogen,

while for the τ nitrogen the pK$_a$=6.92.

For histidine, the titration was similar to the imidazole sigmoidal sharp curve. The difference in pK$_a$ of the two nitrogens was attributed to the alteration of the local electrostatic environment due to the backbone of histidine amino acid, which is also responsible for the differentiation of the two nitrogens (Scheme S9, ESI).

In order to reduce the pK$_a$ of PHIS to endosomal pH, Kim et al.[27] synthesized PEO-*b*-poly(L-histidine-*co*-phenylalanine), where the random addition of the hydrophobic L-phenylalanine along the PHIS chain increased the hydrophobicity and a lower pH was required in order to become hydrophilic. The poly(L-histidine-*co*-phenylalanine) block was synthesized by the copolymerization of N^{im}-benzyl protected N-carboxy anhydride of L-histidine and L-phenylalanine NCA, and the amine end-functionalized copolypeptides were linked with a PEO-NHS ester. The deprotection of N^{im}-benzyl group was performed by the reaction with Na under liquid ammonia. They found that the addition of the PEO chain at the PHIS increased the pK$_a$ by about 0.5 units (7.0 instead of 6.5 for the pure PHIS), while the hydrophobic amino acid phenylalanine (PHE) reduced the pK$_a$ of the copolypeptide by about 0.4 units in 55 % molar ratio of PHE/HIS.

Zelikin et al.[61] determined the pK$_a$ of a PHIS with MW=12.5 x 10^5 g/mol by measuring the interactions with DNA and obtained a pK$_a$=6.24.

In the present work, in order to elucidate the influence of the PEO chain or the hydrophobic amino acids, *γ-benzyl*-L-glutamate or leucine along the PHIS chain of PHIS, on the pK$_a$, compared to the PHIS homopolypeptides, we performed turbidity measurements of the PHIS homopolypeptides and titrations of the PEO-*b*-PHIS, the PEO-*b*-P(HIS-*co*-BLG X) and the PEO-*b*-P(HIS-*co*-LEU-X), with x = 10, 20 and 40. Initially, turbidity measurements were performed on the PHIS homopolypeptides (Figure 19) in order to obtain the pK$_a$ of PHIS 6K along with PHIS 35K. The pK$_a$ is related to pH and the degree of ionization $α$ according to the following equation:

$$pH = pK_a - m \ x \ \log\frac{a}{1-a}$$ (3)

In the middle of the titration curve (Figure 19), half of the monomeric units of the PHIS are ionized, where the others are deprotonated and therefore hydrophobic. At this point, $\alpha = \frac{1}{2}$ and therefore log(a/1-a)=0, and the pH at that point equals pK$_a$. It was found that the pK$_a$ of 6K PHIS was 6.7, while the pK$_a$ of PHIS 35K was 6.4, close to the one obtained for histidine by Donnini et al.[60] (6.54), slightly higher than that obtained by Kim et al,[27] (6.50) and significantly higher than the value obtained by Zelikin et al.[61] (6.24 for a 12.5 x 10^3 g/mol PHIS). It is obvious that pK$_a$ depends on the molecular weight. In addition, the turbidity of the solution of PHIS 6K was significantly higher than that PHIS 35K with the same concentration, indicated by the much higher adsorption at the same concentration and pH. This is due to the better organization of PHIS 6K which forms elongated β-sheets rather than the broken β-sheets of the PHIS 35K that cannot be packed tightly. From the amount of NaOH used to titrate the PHIS homopolymers it was possible to obtain the amount of PHIS in the copolymers (composition) and compare with values obtained by ^{1}H NMR spectroscopy (Figure F16 ESI). Turbidity measurements could not be performed at the PEO-containing copolymers and terpolymers since PEO is soluble in water and kept the co- and terpolymers soluble even at high pH values.

For that purpose, we performed titrations of the PHIS homopolypeptide along with the PEO-*b*-PHIS, PEO-*b*-P(HIS-*co*-LEU-X) (Figure 20) and of the PEO-*b*-P(HIS-*co*-BLG-X) (Figure F17, ESI), so that the number of monomeric units of pure PHIS was always constant. It can be seen that the titration curve of PHIS is not a typical sigmoidal titration curve of a simple base, but it starts to become protonated from pH~3 up to pH~8.5. This difference results in the buffering capacity of PHIS, which binds the protons over a wide pH range rendering the pH of the environment constant, close to its pK$_a$. This difference in the titration curve between the histidine molecule (typical sharp sigmoidal

curve) and poly(L-histidine) is due to its polymeric nature and particularly to its secondary structure, which causes each monomeric block to behave differently depending on the conformation of PHIS.

The pH at the end point of the PHIS homopolymer is a unique value defined by the basicity of PHIS and therefore its pK_a. The difference between the pH at the end point of PHIS homopolymer and the pK_a obtained by the turbidity measurements is compared to the difference between the pH of the homopolymer and the other co-and terpolymers, and since the concentration of pure PHIS is always constant, the difference in pH at the end point is equal to the difference in pK_a of these polymers. The obtained pK_a of the polymers are shown in Table 2. The effect of BLG/PHIS or LEU/PHIS ratio on the pK_a value is given in Figure 21. It is obvious that the more hydrophobic BLG has a higher impact on the reduction of pK_a than that of LEU.

Figure 19

Figure 20

Figure 21

The most impressive result shown in Figure 22 was that close to the pK_a values of each polymer, particularly of the terpolymers with higher amounts of hydrophobic amino acids, addition of solution of 0.01 N NaOH did not significantly change the pH of the solution, resulting in a slight plateau (indicated at the inset of the Figure 22), proving the stronger buffering capacity of these polymers.

In addition to impacting the pK_a of pure PHIS, the LEU and BLG units also effect the shape of the titration curve. The titration curves of PEO-*b*-PHIS as well as PEO-*b*-P(HIS-*co*-LEU-40) polymers are depicted in Figure 22. It can be seen that from pH=3.0 up to pH=6.0, by adding the same amount of NaOH, the pH of the solution of the PEO-*b*-P(HIS-*co*-LEU-40) is higher than that of PEO-

b-PHIS. Consequently, the concentration of free [H$^+$] is higher in the solution of PEO-*b*-PHIS and therefore the amount of protonated HIS is lower, since the total amount of PHIS is the same in both solutions and the amount of added NaOH is also equal. This proves that for PEO-*b*-P(HIS-*co*-LEU-40), the PHIS units are more protonated at lower pH values (such as 5.0 that was tested by DLS) and thus PEO-*b*-P(HIS-*co*-LEU-40) is expected to present lower aggregation at the same pH, compared to the PEO-*b*-PHIS copolymer. It seems that the presence of the hydrophobic amino acids along the PHIS chain render the HIS units more basic probably due to the transition of the secondary structure from *β*-sheet to random coil, even at higher pH values rendering the HIS more susceptible to interaction with water and therefore more protonated, while maintaining the final pH at the end point lower at the terpolymers and also lowering their pK$_a$. This also verifies that LEU and BLG monomeric units are randomly distributed along the PHIS chain, since if P(HIS-*co*-LEU(BLG)-X) were blocky, the titration curve would be similar to that of the copolymer PEO-*b*-PHIS.

The titration curve shows precisely the degree of protonation of PEO-*b*-PHIS as compared to the PEO-*b*-P(HIS-*co*-LEU(BLG)-x), which also reflects the aggregation phenomena discussed below. From 5.8<pH<7.4, the protonation of the terpolymers is lower rendering them more stable and more insoluble. Consequently, in order to avoid the disruption of the aggregates over this pH range, i.e. the extracellular pH of a cancer cell (6.7-6.9), a terpolymer has to be used rather than the PEO-*b*-PHIS. Depending on the amount of hydrophobic peptide along the PHIS chain (LEU or BLG) it is possible to fine-tune the pH at which the aggregate will be disrupted, i.e. at the early endosome. At lower pH values (i.e. late endosomes), the terpolymers disrupt faster than PEO-*b*-PHIS. In addition, the terpolymers have better buffering capacity and maintain the pH at a range from 6.0-6.4, especially when the amount of hydrophobic blocks is higher, making them ideal for the "proton sponge mechanism" where the membrane of the endosomes is ruptured and the drugs are released inside the cytoplasm. Consequently, depending on the desired terpolymer application,

it is possible to fine-tune the point at which the aggregates will be disrupted, a feature very important for drug delivery applications.

Figure 22

Dependence of aggregation of the hybrid diblock and triblock ter-and quarterpolymers on pH and temperature obtained by dynamic light scattering (DLS).

pH Dependence of the aggregation.

In most studies of PHIS-containing amphiphilic polymers where the dimensions of the aggregates are examined as a function of pH, it was found that the dimensions of the aggregates increase at lower pH compared to pH=7.4, due to the protonation of PHIS, which gradually becomes hydrophilic and therefore interacts with water and subsequently swells.[24, 27, 30]

In order to investigate the influence of the water solubility of PHIS with pH, we observed the aggregation phenomena of the diblock co- and terpolymers PEO-*b*-PHIS, PEO-*b*-P(HIS-*co*-BLG-X) and of the PEO-*b*-P(HIS-*co*-LEU-X) along with the triblock terpolymer and quarterpolymer at pH=7.4 and pH=5.0, values within the physiological pH range. The pH values were adjusted using a PBS buffer. One indication of the pH sensitivity of PHIS arises from the ^{1}HNMR spectrum of PEO-*b*-PHIS taken in pure D_2O. Surprisingly, the spectrum contained almost no peaks for PHIS, and when one drop of a 33 % DCl solution in D_2O was added in the same tube, the PHIS peaks appeared with the expected intensity. That indicates that PHIS aggregates in pure water with pH=7.4, but is protonated at lower pH and dissolved in water (Figure F18, ESI).

The results from DLS are illustrated in Table 3. DLS measurements were performed at three different pH values for the PEO-*b*-PHIS, i.e. 7.4, 5.0 and 3.0. The buffer used for the adjustment to pH=3.0 was a potassium biphthalate/sulphamic acid. It is obvious that at pH=5.0 the aggregates are swollen as compared to the one at pH=7.4, due to the change in solubility of PHIS block, that

becomes partially protonated and therefore partially hydrophilic. At pH=3.0, the PHIS block is completely protonated and therefore completely hydrophilic, resulting in complete aggregation disruption. The β-sheet conformation, which developed at pH higher than 5.0 and coexists with the random coil conformation even at lower pH values, keeps the PHIS chains aggregated, and only when the pH drops to 3.0 where the PHIS monomeric units are completely protonated and with the random coil conformation, the aggregation is completely disrupted.

In case of the PEO-*b*-P(HIS-*co*-BLG-X), the aggregates formed are relatively large to be typical core-shell micelles, and probably form vesicular structures. The results indicate that the aggregates become more condensed upon increasing the amount of BLG from 10 to 40 %. At pH=5.0 they become swollen, and the dimensions of the aggregates increase. However, the KCounts of the scattering light are lower at pH=5.0, also indicating partial disruption of the aggregates. For the PEO-*b*-P(HIS-*co*-LEU-X) terpolymers at pH=7.4, it is obvious that the aggregates become more condensed when the amount of LEU increases from 10 to 40 %. Surprisingly, the aggregates become completely disrupted at pH=5.0, particularly when the amount of LEU is highest (40 %), a phenomenon not observed for the PHIS homopolypeptide where complete disruption occurs at lower pH. This is in agreement with the titration curves obtained where we found that at pH=5.0 the degree of protonation of PHIS is higher in case of PEO-*b*-P(HIS-*co*-LEU-40), slightly lower at the PEO-*b*-P(HIS-*co*-BLG-40) and the lowest at the PEO-*b*-PHIS.

In case of the triblock terpolymer PEO-*b*-PHIS-*b*-PLL, it is obvious that the connection of a PEO-*b*-PHIS with the PLL leads to increased pH sensitivity, since at pH=5.0 significant disruption is observed. However, the presence of only 15 % molar ratio of BLG in the PEO-*b*-P(HIS-*co*-BLG-15)-*b*-PLL quarterpolymer maintains the aggregation and the protonation of HIS at pH=5.0 results only in swollen aggregates. In both triblocks, the aggregates at pH=7.4 are probably vesicles, since they too large to be simple core-shell micelles.

Dependence of PEO-*b*-PHIS Aggregation as a Function of Temperature

In order to examine the influence of the transition in conformation of low molecular weight PHIS to its aggregation, 3 mg of PEO-*b*-PHIS were dissolved in 3 mL of MilliQ water and the pH was adjusted at 7.40 by the addition of a small amount of a 0.1 N NaOH solution in water. The results of DLS at 25, 37 and 50 ^{o}C are shown in Table 4. It is obvious that the increase of temperature has the same impact with the lowering of pH, i.e. the aggregates become swollen since their dimensions increase and the KCounts diminish. This implies that the increase in temperature makes the PHIS more soluble in water, probably due to the conformation transition from a *β*-sheet probably to an interrupted *β*-sheet conformation. The highly developed *β*-sheet conformation of PHIS at lower temperatures results to better packing between itself as compared to the broken *β*-sheets at higher temperatures, resulting in lower aggregation. This is also supported by the higher turbidity obtained for the PHIS 6K homopolypeptide, compared to the PHIS 35, indicating better organization of the hydrophobic PHIS segments and better packing of the low molecular weight extended *β*-sheets.

Conclusions

We present the synthesis of the novel monomer *Trt*-HIS-NCA. The trityl group is a versatile group which can be orthogonally deprotected under mildly acidic conditions leaving intact other groups, such as benzyl ester, that deprotect under stronger acidic conditions, or that deprotect under basic conditions. In addition, it presents the lowest racemization during deprotection. Kinetic studies of the *Trt*-His-NCA showed first order kinetics, indicating that the polymerization follows the normal amine mechanism, and *Trt*-His-NCA was found to polymerize more slowly than BLG-NCA or BOCLL-NCA. The high purity of the NCA along with the use of the high vacuum techniques

led to the synthesis of novel well-defined amphiphilic fully polypeptidic as well as hybrid polymers in a variety of macromolecular architectures. The combined characterization results revealed that the polymers exhibited very high degree of molecular and compositional homogeneity despite their complexity. The synthesis of highly pure sarcosine-NCA along with copolypeptides with PHIS is also presented.

It was found that the secondary structure is the key parameter that defines the aggregation properties of the PHIS block. The secondary structure of PHIS obtained by Circular Dichroism revealed a random coil conformation at pH values lower than 5.0, while the β-sheet conformation is most likely adopted at higher pH values for the PHIS homopolypeptide. At low molecular weights PHIS is not only pH-responsive, but is also temperature responsive, since the β-sheet transforms to a broken β-sheet conformation. The study of the presence of PLEU randomly distributed along the PHIS chain as a function of LEU molar ratio and pH revealed that LEU hinders the organization of PHIS at higher pH where it deprotonates, maintaining some random coil conformation at every pH and LEU composition, resulting in the more facile protonation-deprotonation of these sequences and providing an explanation as to why the PEO-*b*-P(HIS-*co*-LEU(BLG)-X) terpolymers presented higher degrees of protonation compared to the PHIS homopolypeptide at the PEO-*b*-PHIS.

The titration results of the PEO-*b*-P(HIS-*co*-LEU(BLG)-X) revealed that LEU and BLG amino acids reduce the pK$_a$ of PHIS. Surprisingly, it was found that the degree of protonation of the PEO-*b*-P(HIS-*co*-LEU(BLG)-X) at pH lower than 5.8 is higher than that of the corresponding PEO-*b*-PHIS, while this was reversed at higher pH values. This study allows for the fine tuning of the pK$_a$ and of the degree of protonation depending on the molecular characteristics of the terpolymers. This is very crucial for drug and gene delivery applications, where the rupture of the aggregates is requisite for the release of drugs and genes in certain subcellular compartments.

The aggregation of the PEO-*b*-P(HIS-*co*-LEU(BLG)-X) and PEO-*b*-PHIS at pH=7.4 and 5.0 confirmed the observations of the titration study, where at pH=5.0 the copolymer swells due to the partial protonation of PHIS which turns partially hydrophilic, maintaining the degree of aggregation, while for the terpolymers at the same pH, swelling is also observed with concurrent disruption of the aggregates due to higher degree of protonation. The same phenomenon appeared by increasing the temperature at pH=7.4 on the PEO-*b*-PHIS copolymers, never reported before. The swelling at higher temperatures is attributed to the transition of the secondary structure from β-sheet to broken β-sheet, preventing dense packing to form stronger aggregates.

The systematic study presented in this work elucidates the secondary structure-protonation degree as well as the pH and temperature dependence of the aggregation of PHIS. This work opens avenues for the synthesis of multifunctional polymers containing this remarkable material, along with the synthesis of PHIS copolypeptides that can allow for the fine tuning of the pH where the aggregates will be disrupted, leading to the control of the rate of and choice of cellular compartment for the drug release. This is tremendously useful for the design of pH- and temperature stimuli material that will be effectively utilized for drug and gene delivery applications and theranostics.

Acknowledgements

Electronic supplementary information (ESI)

Electronic supplementary information (ESI) available: Schemes depicting the synthesis of the NCAs, Figures showing ^{1}H NMR spectra of NCAs, calibration curves for kinetic measurements, size exclusion chromatograms of diblock copolymer PSAR-b-PHIS as well as diblock terpolymers.

Corresponding Author

Corresponding author: Hermis Iatrou, Email: iatrou@chem.uoa.gr.

Abbreviations

BLG-NCA, *γ-benzyl*-L-glutamate N-carboxy anhydride; BOCLL-NCA, ε-tert-butyloxycarbonyl-L-Lysine N-carboxy anhydride; n-BuLi, n-Butyl lithium; CD, Circular dichroism; DDS, Drug Delivery Systems; DLS, Dynamic Light Scattering**;** DMA, Dimethylamine; *Trt*-HIS-NCA, N^{im} trityl protected N-carboxy anhydride of L-histidine; HVT, High vacuum techniques; LEU, L-leucine; LEU-NCA, L-Leucine N-carboxy anhydride; PEO, poly(ethylene oxide); PHIS, poly(L-histidine); PLL, poly(L-lysine hydrochloride); PBLG, poly(*γ-benzyl*-L-glutamate); SAR-NCA, sarcosine N-carboxy anhydride; SEC, Size-exclusion chromatography; TFA, Trifluoroacetic acid; ROP, Ring Opening Polymerization;

Table 1. Molecular Characteristics of the Synthesized Polymers

Polymer	M_n 1st Block x 10^{-3a}	M_n 2nd Block x 10^{-3b}	M_n 3rd Block x 10^{-3c}	Stoich. M_n x 10^{-3d}	Total M_n x 10^{-3e}	I^f	Composition % (w/w)
PHIS 6K	6.1	-	-	6.0		1.12	-
PHIS 35K	36.3	-	-	35.0		1.23	-
PEO-*b*-PHIS	9.95	5.80	-	16.0	15.8	1.11	PEO/PHIS: 63/37
PEO-*b*-P(HIS-*co*-BLG 10)	9.95	5.75	-	16.0	15.7	1.12	PEO/HIS/BLG: 63/33/4
PEO-*b*-P(HIS-*co*-BLG 20)	9.95	5.60	-	16.0	15.6	1.10	PEO/HIS/BLG: 63/28/9
PEO-*b*-P(HIS-*co*-BLG 40)	9.95	5.90	-	16.0	15.9	1.14	PEO/HIS/BLG: 63/20/17
PEO-*b*-P(HIS-*co*-LEU 10)	9.95	5.70	-	16.0	15.6	1.10	PEO/HIS/LEU: 63/35/2
PEO-*b*-P(HIS-*co*-LEU 20)	9.95	6.00	-	16.0	15.6	1.09	PEO/HIS/LEU: 63/32/5
PEO-*b*-P(HIS-*co*-LEU 40)	9.95	6.00	-	16.0	16.0	1.17	PEO/HIS/LEU: 63/27/10
PSAR-*b*-PHIS 1	4.26	2.50	-	6.0	6.8	1.11	PSAR/PHIS: 63/37
PSAR-*b*-PHIS 2	10.8	8.50	-	20.0	19.3	1.13	PSAR/PHIS: 56/44
PEO-*b*-PHIS-*b*-PLL	9.95	5.90	5.0	22.0	20.9	1.21	PEO/PHIS/PLL: 48/28/24
PEO-*b*-P(HIS-*co*-BLG 15)-*b*-PLL	9.95	6.10	4.80	22.0	20.9	1.20	PEO/PHIS/PLL/BLG: 48/26/23/3
PBLG-*b*-(PLL-*g*-*Trt*-PHIS)	22.1	1.30	10 arms x 1.50	40.0	38.4	1.12	PBLG/PLL/P(*Trt*-HIS): 58/3/39

[a]Obtained by SEC-TALLS.

[b]Obtained by the difference between the molecular weight of the first block and the diblock obtained by SEC-TALLS.

[c]Obtained by the difference between the molecular weight of the diblock and the triblock obtained by SEC-TALLS. In case of the graft we consider that all ε-amines (10 per polymeric chain) of poly(L-lysine) participates in the polymerization of *Trt*-HIS-NCA.

[d]Stoichiometric molecular weight.

[e]Molecular weight of the final polymer obtained by SEC-TALLS.

[f]Polydispersity index obtained by SEC.

Table 2. pK$_a$ Dependence as a Function of Molar Ratio of Hydrophobic Amino Acid.

Polymer	% mol BLG or LEU	pH at the end point	pK$_a$
PHIS 35K	0	8.00	6.4
PHIS 6K	0	8.03	6.7
PEO-*b*-PHIS	0	8.06	6.73
PEO-*b*-P(HIS-*co*-BLG 10)	10 BLG	7,83	6.5
PEO-*b*-P(HIS-*co*-BLG 20)	20 BLG	7,27	5.94
PEO-*b*-P(HIS-*co*-BLG 40)	40 BLG	7,20	5.87
PEO-*b*-P(HIS-*co*-LEU 10)	10 LEU	7.82	6.49
PEO-*b*-P(HIS-*co*-LEU 20)	20 LEU	7.57	6.24
PEO-*b*-P(HIS-*co*-LEU 40)	40 LEU	7.38	6.05

Table 3. DLS results of the Diblock and Triblock Polymers at pH=7.4 and 5.0 adjusted with a PBS Buffer.

Sample	pH=7.4			pH=5.0			pH=3.0		
	R_H (nm)	Poly	KCounts	R_H (nm)	Poly	KCounts	R_H (nm)	Poly	KCounts
PEO-*b*-PHIS	54.6	0.48	10.3	180	0.19	11	No signal	No signal	No signal
PEO-*b*-P(HIS-*co*-BLG 10)	99.3	0.39	70.9	605	0.60	28.6			
PEO-*b*-P(HIS-*co*-BLG 20)	120.0	0.67	75	257	0.36	58			
PEO-*b*-P(HIS-*co*-BLG 40)	68.8	0.40	30	36.1	0.80	21			
PEO-*b*-P(HIS-*co*-LEU 10)	180	0.48	123	169.6	0.23	5.8			
PEO-*b*-P(HIS-*co*-LEU 20)	94.0	0.54	28	237	0.09	5.4			
PEO-*b*-P(HIS-*co*-LEU 40)	40.0	0.18	10.4	No signal	No signal	No signal			
PEO-*b*-PHIS-*b*-PLL	112	0.26	78.1	179	0.82	7.0			
PEO-b-P(HIS-*co*-BLG 15)-*b*-PLL	159	0.38	66.5	257	0.26	61			

Table 4. DLS Results of the Diblock PEO-*b*-PHIS at pH=7.40 and T=25, 37 and 50 ^{o}C adjusted with a 0.1 N Water Solution of NaOH.

	PEO-*b*-PHIS at pH=7.4		
Temperature (^{o}C)	R_H (nm)	Poly	KCounts
25	29.8	0.15	60.1
37	37.0	0.13	48.5
50	43.3	0.17	42.6

References

1. C. F. Higgins, *Nature*, 2007, **446**, 749-757.
2. G. Kibria, H. Hatakeyama and H. Harashima, *Archives of pharmacal research*, 2014, **37**, 4-15.
3. E. Gullotti and Y. Yeo, *Molecular Pharmaceutics*, 2009, **6**, 1041-1051.
4. B. A. Webb, M. Chimenti, M. P. Jacobson and D. L. Barber, *Nature reviews. Cancer*, 2011, **11**, 671-677.
5. F. A. Gallagher, M. I. Kettunen, S. E. Day, D. E. Hu, J. H. Ardenkjaer-Larsen, R. Zandt, P. R. Jensen, M. Karlsson, K. Golman, M. H. Lerche and K. M. Brindle, *Nature*, 2008, **453**, 940-943.
6. A. Patchornik, A. Berger and E. Katchalski, *Journal of the American Chemical Society*, 1957, **79**, 5227-5230.
7. D. W. Pack, D. Putnam and R. Langer, *Biotechnology and Bioengineering*, 2000, **67**, 217-223.
8. D. J. Chen, B. S. Majors, A. Zelikin and D. Putnam, *Journal of controlled release : official journal of the Controlled Release Society*, 2005, **103**, 273-283.
9. D. Putnam, C. A. Gentry, D. W. Pack and R. Langer, *Proceedings of the National Academy of Sciences of the United States of America*, 2001, **98**, 1200-1205.
10. D. Putnam, A. N. Zelikin, V. A. Izumrudov and R. Langer, *Biomaterials*, 2003, **24**, 4425-4433.
11. F. Aldeek, M. Safi, N. Zhan, G. Palui and H. Mattoussi, *Acs Nano*, 2013, **7**, 10197-10210.
12. W. R. Algar, D. E. Prasuhn, M. H. Stewart, T. L. Jennings, J. B. Blanco-Canosa, P. E. Dawson and I. L. Medintz, *Bioconjugate chemistry*, 2011, **22**, 825-858.
13. Y. Jin and X. Gao, *Journal of the American Chemical Society*, 2009, **131**, 17774-17776.
14. D. E. Prasuhn, J. B. Blanco-Canosa, G. J. Vora, J. B. Delehanty, K. Susumu, B. C. Mei, P. E. Dawson and I. L. Medintz, *Acs Nano*, 2010, **4**, 267-278.
15. Y. Jin, *Accounts of Chemical Research*, 2014, **47**, 138-148.
16. C.-H. Lu, Y.-F. Lin, J.-J. Lin and C.-S. Yu, *Plos One*, 2012, **7**.
17. J. W. Lee and J. D. Helmann, *Nature*, 2006, **440**, 363-367.
18. A. N. Zelikin, E. S. Trukhanova, D. Putnam, V. A. Izumrudov and A. A. Litmanovich, *Journal of the American Chemical Society*, 2003, **125**, 13693-13699.
19. J. Kovacs, S. Kim, E. Holleran and P. Gorycki, *Journal of Organic Chemistry*, 1985, **50**, 1497-1504.
20. S. Terada, A. Kawabata, N. Mitsuyasu, H. Aoyagi and N. Izumiya, *Bulletin of the Chemical Society of Japan*, 1978, **51**, 3409-3410.
21. J. M. Benns, J. S. Choi, R. I. Mahato, J. S. Park and S. W. Kim, *Bioconjugate chemistry*, 2000, **11**, 637-645.
22. S. Asayama, H. Kawakami and S. Nagaoka, *Polymers for Advanced Technologies*, 2004, **15**, 439-444.
23. K. T. Oh and E. S. Lee, *Polymers for Advanced Technologies*, 2008, **19**, 1907-1913.
24. J. H. Hwang, C. W. Choi, H. W. Kim, H. Kim do, T. W. Kwak, H. M. Lee, C. H. Kim, C. W. Chung, Y. I. Jeong and D. H. Kang, *International journal of nanomedicine*, 2013, **8**, 3197-3207.
25. H. Wu, L. Zhu and V. P. Torchilin, *Biomaterials*, 2013, **34**, 1213-1222.
26. E. S. Lee, H. J. Shin, K. Na and Y. H. Bae, *Journal of Controlled Release*, 2003, **90**, 363-374.
27. G. M. Kim, Y. H. Bae and W. H. Jo, *Macromolecular bioscience*, 2005, **5**, 1118-1124.
28. R. P. Johnson, Y.-I. Jeong, E. Choi, C.-W. Chung, D. H. Kang, S.-O. Oh, H. Suh and I. Kim, *Advanced Functional Materials*, 2012, **22**, 1058-1068.
29. W. Park, D. Kim, H. C. Kang, Y. H. Bae and K. Na, *Biomaterials*, 2012, **33**, 8848-8857.
30. R. P. Johnson, Y. I. Jeong, J. V. John, C. W. Chung, D. H. Kang, M. Selvaraj, H. Suh and I. Kim, *Biomacromolecules*, 2013, **14**, 1434-1443.
31. J. S. Choi, E. J. Lee, S. J. Park, H. J. Kim and J. S. Park, *Bulletin of the Korean Chemical Society*, 2001, **22**, 261-262.
32. T. Aliferis, H. Iatrou and N. Hadjichristidis, *Biomacromolecules*, 2004, **5**, 1653-1656.
33. N. Hadjichristidis, H. Iatrou, M. Pitsikalis and G. Sakellariou, *Chemical Reviews*, 2009, **109**, 5528-5578.

34. M. Gkikas, B. P. Das, M. Tsianou, H. Iatrou and G. Sakellariou, *European Polymer Journal*, 2013, **49**, 3095-3103.
35. M. Gkikas, H. Iatrou, N. S. Thomaidis, P. Alexandridis and N. Hadjichristidis, *Biomacromolecules*, 2011, **12**, 2396-2406.
36. M. Gkikas, J. Timonen, J. Ruokolainen, P. Alexandridis and H. Iatrou, *Journal of Polymer Science Part A: Polymer Chemistry*, 2013, **51**, 1448-1456.
37. R. Graf, H. W. Spiess, G. Floudas, H. J. Butt, M. Gkikas and H. Iatrou, *Macromolecules*, 2012, **45**, 9326-9332.
38. T. J. Deming and S. A. Curtin, *Journal of the American Chemical Society*, 2000, **122**, 5710-5717.
39. X. Sun, G. Yu, Q. Xu, N. Li, C. Xiao, X. Yin, K. Cao, J. Han and Q. Y. He, *Metallomics : integrated biometal science*, 2013, **5**, 928-935.
40. Y. Wu, G. Chang, Y. Zhao and Y. Zhang, *Dalton transactions*, 2014, **43**, 779-783.
41. M. Peana, S. Medici, V. M. Nurchi, G. Crisponi, J. I. Lachowicz and M. A. Zoroddu, *Dalton transactions*, 2013, **42**, 16293-16301.
42. S. V. Wegner and J. P. Spatz, *Angewandte Chemie*, 2013, **52**, 7593-7596.
43. P. Sieber and B. Riniker, *Tetrahedron Letters*, 1987, **28**, 6031-6034.
44. N. Hadjichristidis, H. Iatrou, S. Pispas and M. Pitsikalis, *Journal of Polymer Science Part A-Polymer Chemistry*, 2000, **38**, 3211-3234.
45. H. Iatrou, H. Frielinghaus, S. Hanski, N. Ferderigos, J. Ruokolainen, O. Ikkala, D. Richter, J. Mays and N. Hadjichristidis, *Biomacromolecules*, 2007, **8**, 2173-2181.
46. M. Mondeshki, H. W. Spiess, T. Aliferis, H. Iatrou, N. Hadjichristidis and G. Floudas, *European Polymer Journal*, 2011, **47**, 668-674.
47. C. Fetsch, A. Grossmann, L. Holz, J. F. Nawroth and R. Luxenhofer, *Macromolecules*, 2011, **44**, 6746-6758.
48. H. Yin, H. C. Kang, K. M. Huh and Y. H. Bae, *Journal of materials chemistry*, 2012, **22**, 91968-19178.
49. H. R. Kricheldorf, *Makromolekulare Chemie-Macromolecular Chemistry and Physics*, 1977, **178**, 1959-1970.
50. K. D. Kopple, *Journal of the American Chemical Society*, 1957, **79**, 662-664.
51. K. D. Kopple, *Journal of the American Chemical Society*, 1957, **79**, 6442-6446.
52. M. Fridkin and S. Shaltiel, *Archives of Biochemistry and Biophysics*, 1971, **147**, 767-&.
53. I. Dimitrov and H. Schlaad, *Chemical Communications*, 2003, 2944-2945.
54. R. P. Johnson, E. Choi, K. M. Lee, S. J. Yu, H. C. Chang, H. Suh and I. Kim, *Microfluidics and Nanofluidics*, 2012.
55. R. Liu, B. He, D. Li, Y. Lai, J. Z. Tang and Z. Gu, *Polymer*, 2012, **53**, 1473-1482.
56. E. S. Lee, K. T. Oh, D. Kim, Y. S. Youn and Y. H. Bae, *Journal of controlled release : official journal of the Controlled Release Society*, 2007, **123**, 19-26.
57. Y. P. Myer and E. A. Barnard, *Archives of Biochemistry and Biophysics*, 1971, **143**, 116-&.
58. E. Peggion, A. Cosani, Terbojev.M and E. Scoffone, *Macromolecules*, 1971, **4**, 725-&.
59. A. V. Finkelstein and O. B. Ptitsyn, *Journal of Molecular Biology*, 1976, **103**, 15-24.
60. S. Donnini, F. Tegeler, G. Groenhof and H. Grubmuller, *Journal of chemical theory and computation*, 2011, **7**, 1962-1978.
61. A. N. Zelikin, E. S. Trukhanova, D. Putnam, V. A. Izumrudov and A. A. Litmanovich, *Journal of the American Chemical Society*, 2003, **125**, 13693-13699.

Figure Captions

Scheme 1. Reactions used in the synthesis of *Trt*-HIS-NCA.

Figure 1. Monitoring the synthesis of *Trt*-HIS-NCA by FT-IR spectroscopy: a) N^α-Boc-$N^{(im)}$-trityl-L-histidine in THF b) After the addition of thionyl chloride formation of NCA peaks at 1780 & 1850 cm$^-$ ^{1} and reduction of 1710 cm^{-1} c) After 2 hours of reaction d) NCA salt after (Et)$_2$O precipitation with characteristic peak of imidazole chloride vibration at 1620 cm^{-1} e) Pure NCA salt after recrystallization with EtAc f) Final *Trt*-His-NCA free of HCl salt and precursor.

Scheme 2. The polymers synthesized: PHIS, PEO-*b*-PHIS, PEO-*b*-P(HIS-*co*-LEU-X), PEO-*b*-P(HIS-*co*-BLG-X).

Scheme 3. The polymers synthesized: PSAR-*b*-PHIS, PEO-*b*-PHIS-*b*-PLL, PEO-*b*-P(HIS-*co*-BLG-15)-*b*-PLL, PBLG-*b*-P(LL-*g*-*Trt*-HIS).

Scheme 4. Reactions used for the synthesis of PEO-*b*-PHIS copolymer.

Scheme 5. Reactions used for the synthesis of the PEO-*b*-P(HIS-*co*-BLG) hybrid terpolymer.

Scheme 6. Reactions used for the synthesis of PEO-*b*-P(HIS-*co*-LEU-X) hybrid block terpolymer.

Scheme 7. Reactions used for the synthesis of PSAR-*b*-PHIS block copolypeptide.

Scheme 8. Reaction scheme for the synthesis of PEO-*b*-P(HIS-*co*-BLG-15)-*b*-PLL triblock quarterpolymer.

Scheme 9. Reactions used for the synthesis of the PBLG-*b*-(PLL-*g*-P(*Trt*-HIS)) block-graft terpolypetide.

Figure 2. ^{1}H NMR spectrum of *Trt*-HIS-NCA HCl salt in CDCl$_3$.

Figure 3. ^{1}H NMR spectrum of the pure *Trt*-HIS-NCA CDCl$_3$.

Figure 4. Monomer consumption as a function of time for different monomer to initiator ratios equal to 20 (black line and points), 50 (red line), 100 (blue line) and 200 (green line). First-order time conversion plots of the HIS-NCA polymerization in DMF initiated by dimethylamine, for DP=20, 50,100,200 and the respective t$_{1/2}$= 0.8, 2.3, 4.5 and 9.6h.

Figure 5. K$_{obs}$ as a function of initiator concentration, for constant monomer concentration.

Figure 6. ^{1}H NMR of the Poly(L-histidine) in D$_2$O and 1 drop of 33 % DCl in D$_2$O.

Figure 7. ^{1}H NMR spectrum of the PEO-*b*-PHIS hybrid copolymer in D$_2$O+DCl.

Figure 8. ^{1}H NMR spectrum of the PEO-*b*-P(HIS-*co*-BLG-20) hybrid copolymer DMSO-*d6* and a drop of D$_2$O+DCl.

Figure 9. ^{1}H NMR spectrum of the PEO-*b*-P(HIS-*co*-BLG-20) hybrid copolymer in deuterated TFA.

Figure 10. ^{1}H NMR spectrum of the PEO-*b*-P(HIS-*co*-BLG-15)-*b*-PLL hybrid copolymer in deuterated DMSO and a drop of D$_2$O+DCl.

Figure 11. SEC eluograms of the synthesis of the PBLG-*b*-(PLL-*g*-P(*Trt*-HIS)) hybrid terpolymer.

Figure 12. ^{1}H NMR spectrum of the PBLG-*b*-(PLL-g-P(*Trt*-HIS)) terpolymer in deuterated DMSO.

Figure 13. CD of PEO-*b*-PHIS copolymer as a function of pH.

Scheme 10. Schematic representation of the conformation of PHIS as a function of pH and molecular weight.

Figure 14. Temperature dependence of the PHIS 6K conformation.

Figure 15. pH dependence of the PHIS 35K conformation.

Figure 16. CD of PEO-*b*-P(HIS-*co*-LEU-10) as a function of pH.

Figure 17. CD of PEO-*b*-P(HIS-*co*-LEU-20) as a function of pH.

Figure 18. CD of PEO-*b*-P(HIS-*co*-LEU-40) as a function of pH.

Figure 19. Turbidity measurement of PHIS 6K to obtain the pK_a=6.7, and of PHIS 35K to obtain a pK_a=6.4.

Figure 20. Titration curves of PEO-*b*-PHIS, and PEO-*b*-P(HIS-*co*-LEU-X) with X = 10, 20 and 40.

Figure 21. Dependence of pK_a of PHIS on the % molar ratio of LEU and BLG.

Figure 22. Degree of protonation of PEO-*b*-PHIS, PEO-*b*-P(HIS-*co*-BLG-40) and PEO-*b*-P(HIS-*co*-LEU-40) as a function of pH.
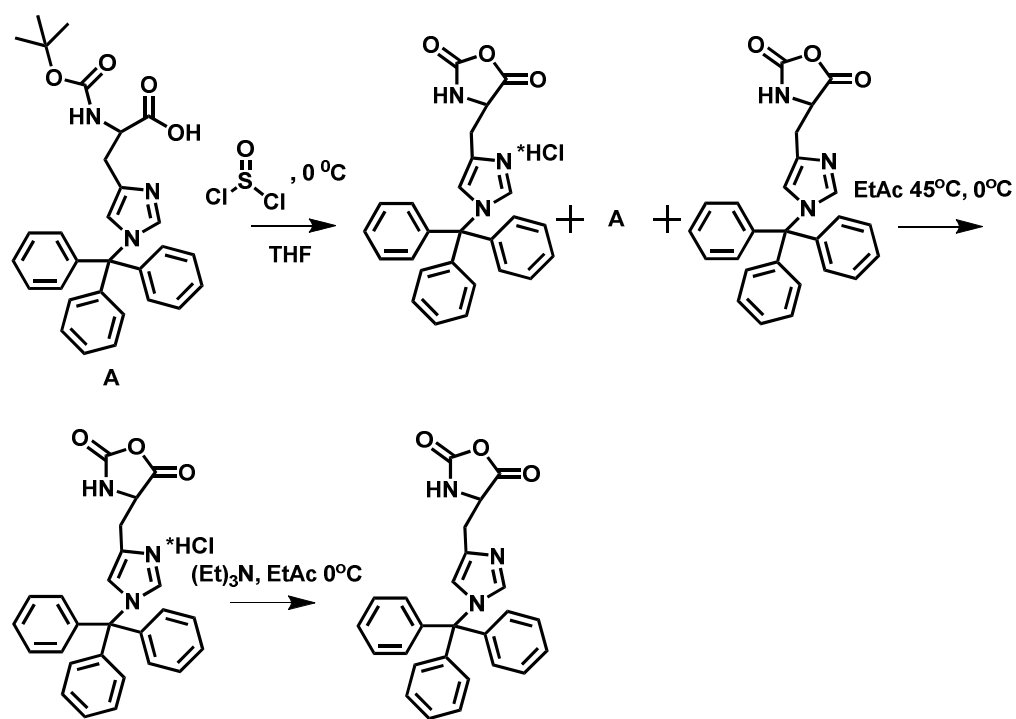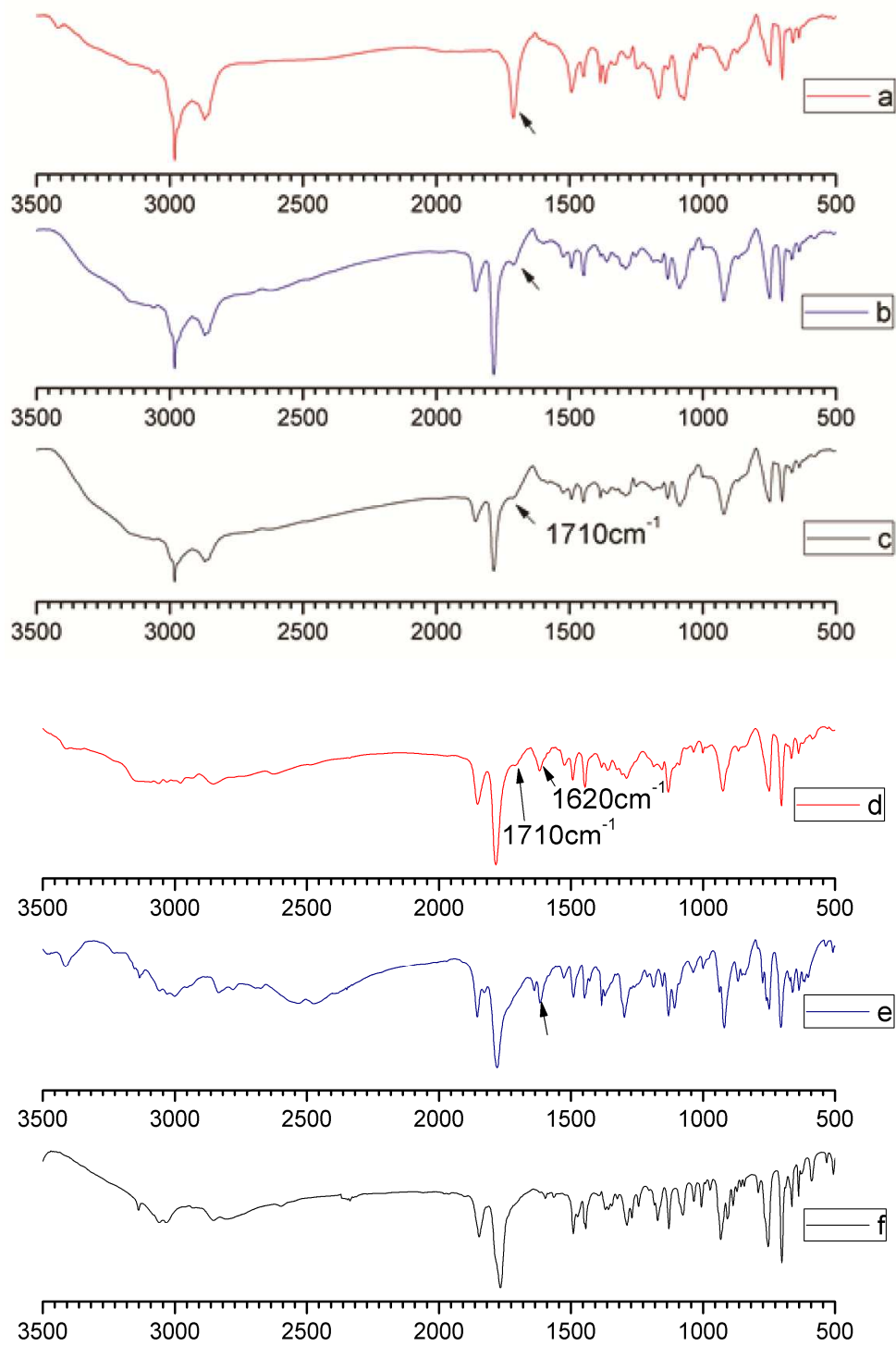
Scheme 1

Figure 1
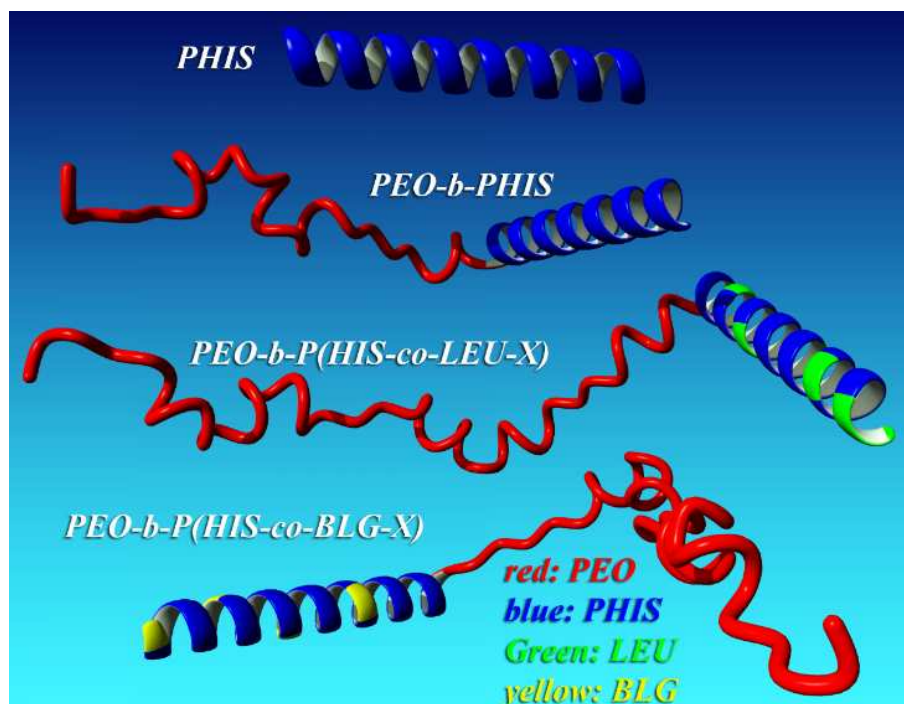
Scheme 2
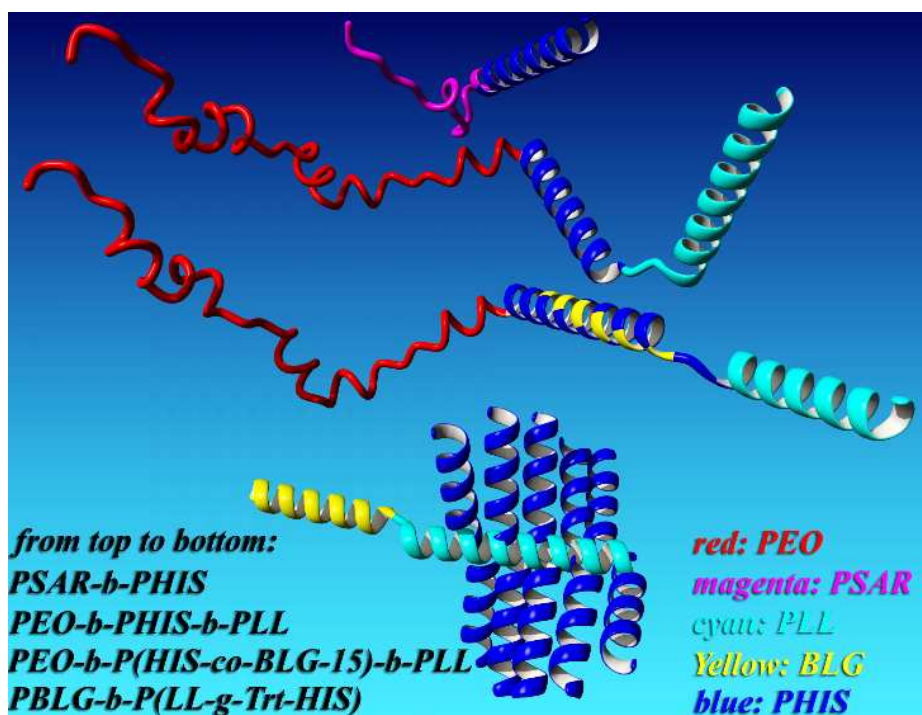
Scheme 3
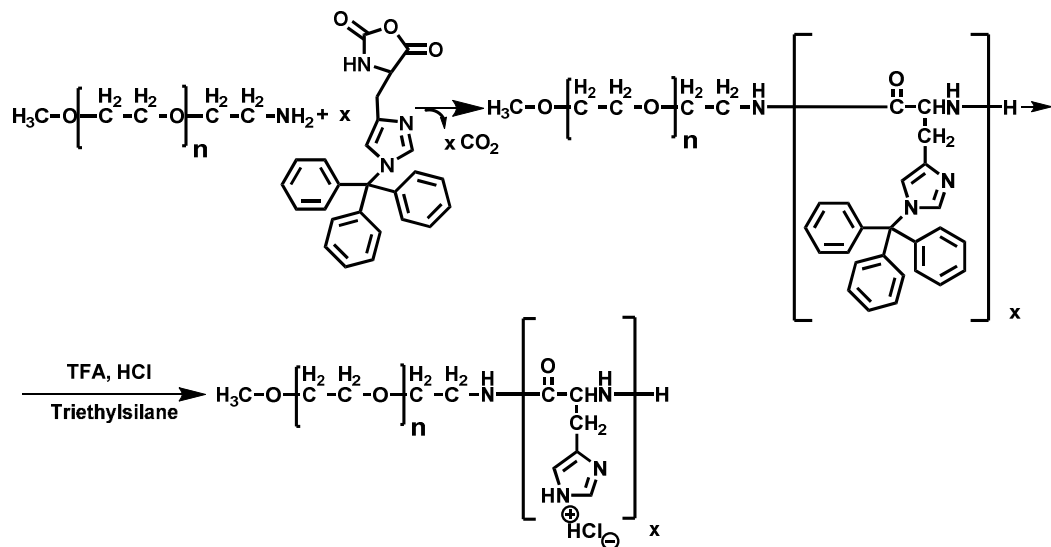
Scheme 4
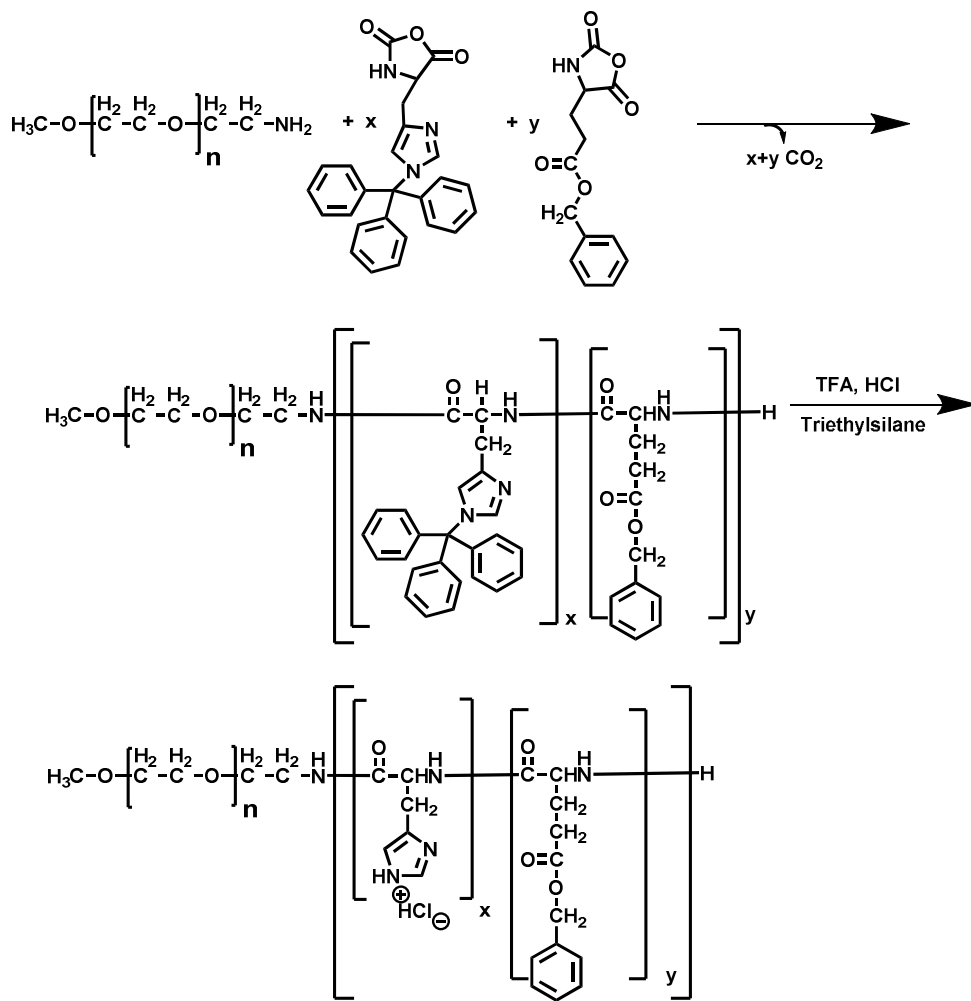
Scheme 5
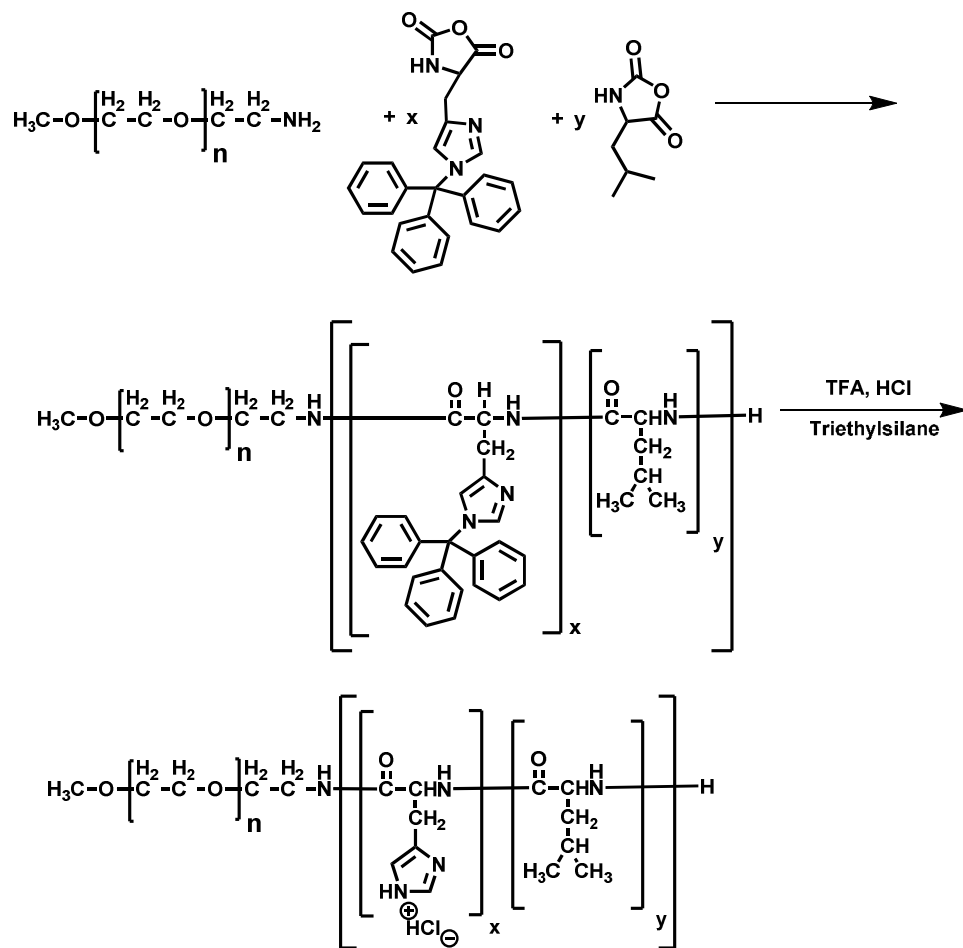
Scheme 6
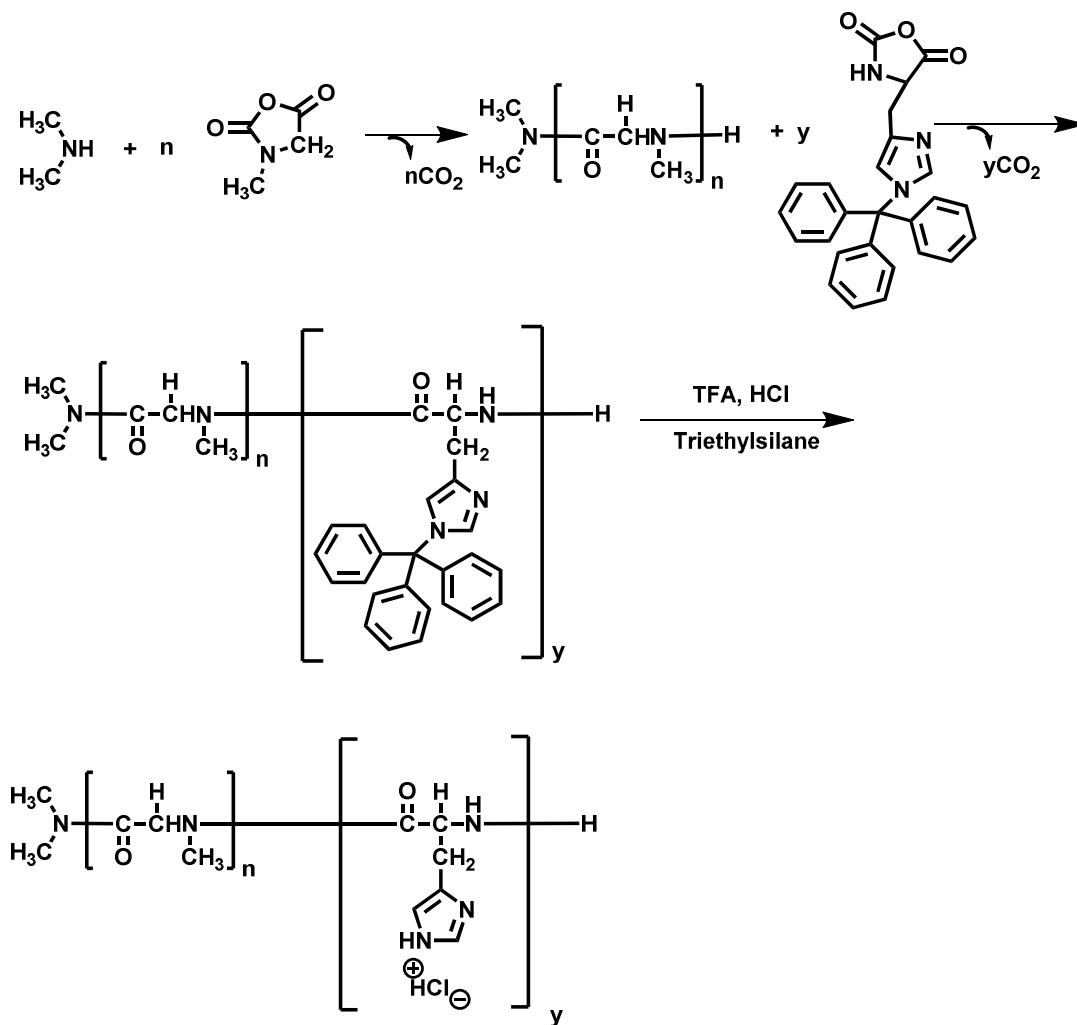
Scheme 7
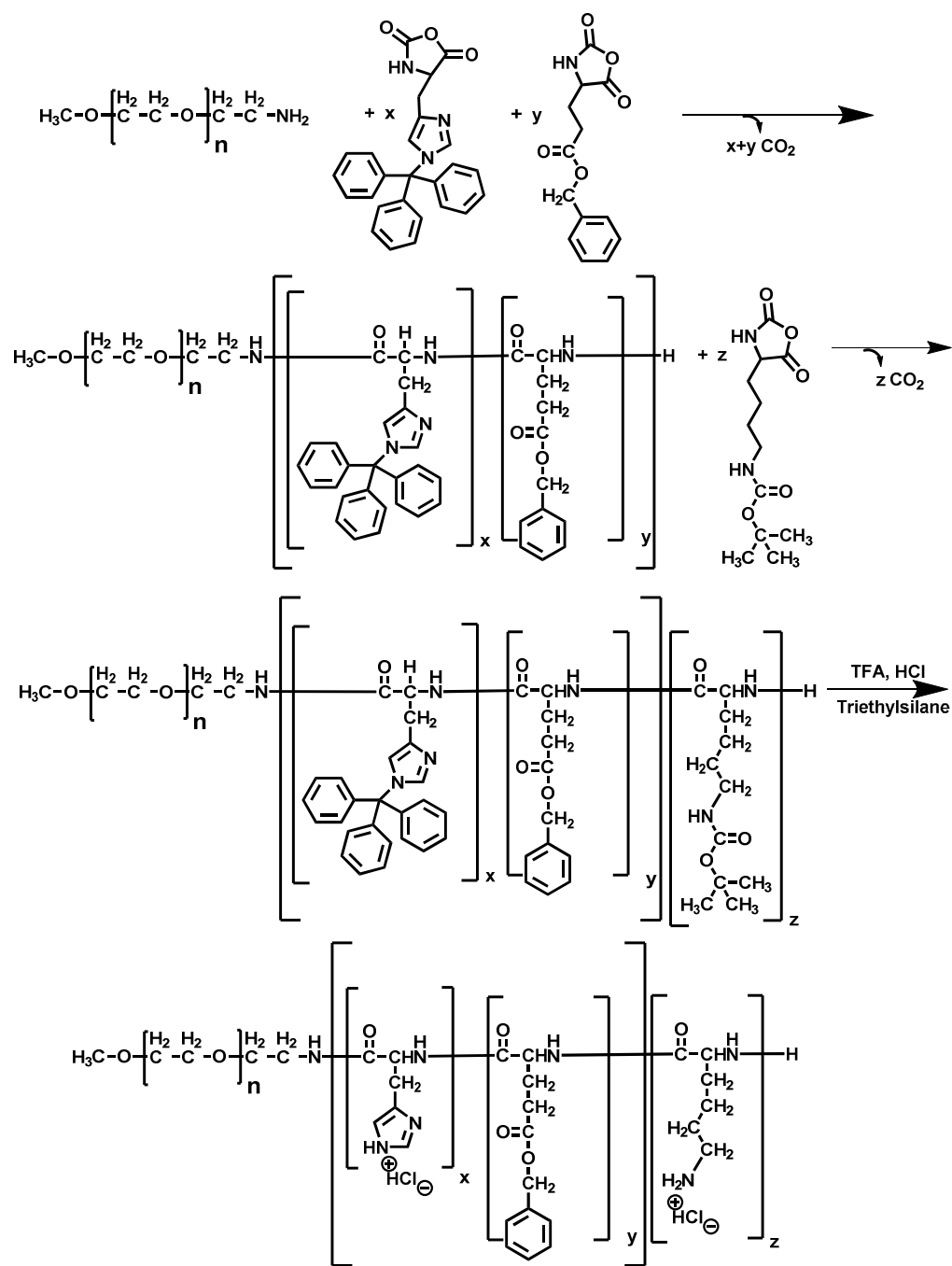
Scheme 8
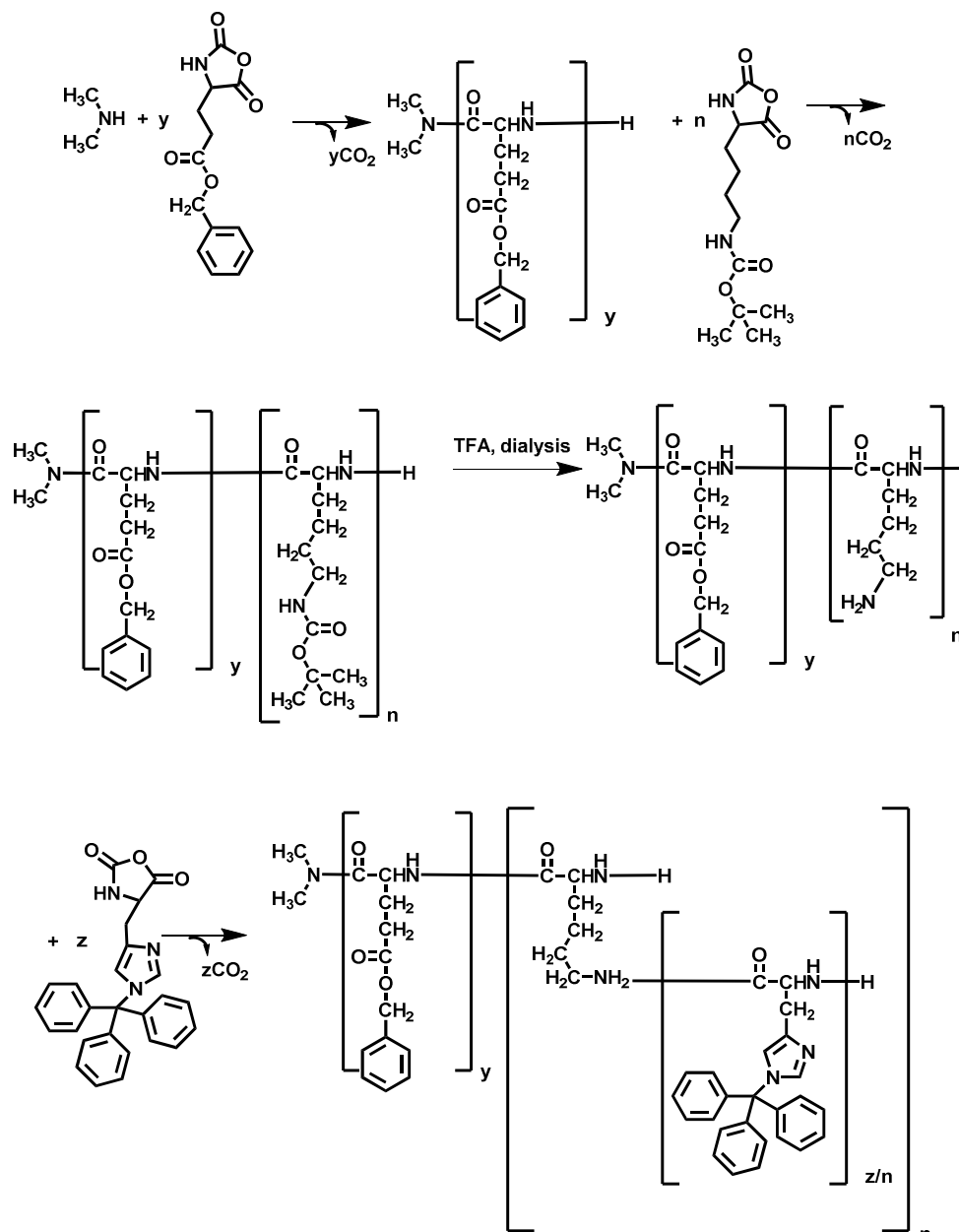
Scheme 9

Figure 2

Figure 3

52

Polymer Chemistry
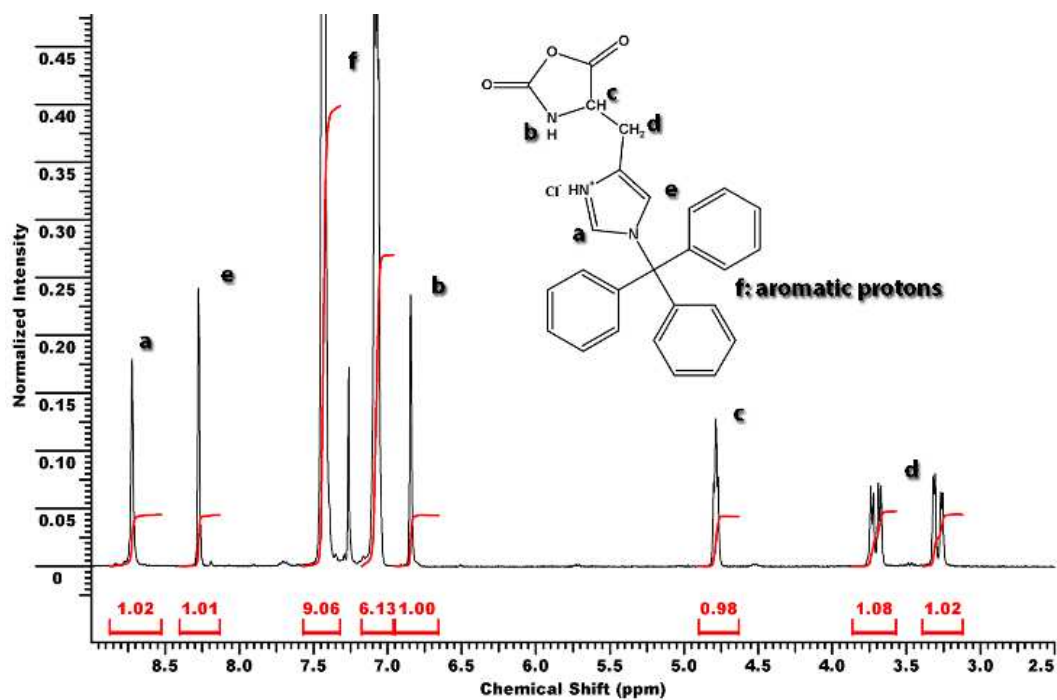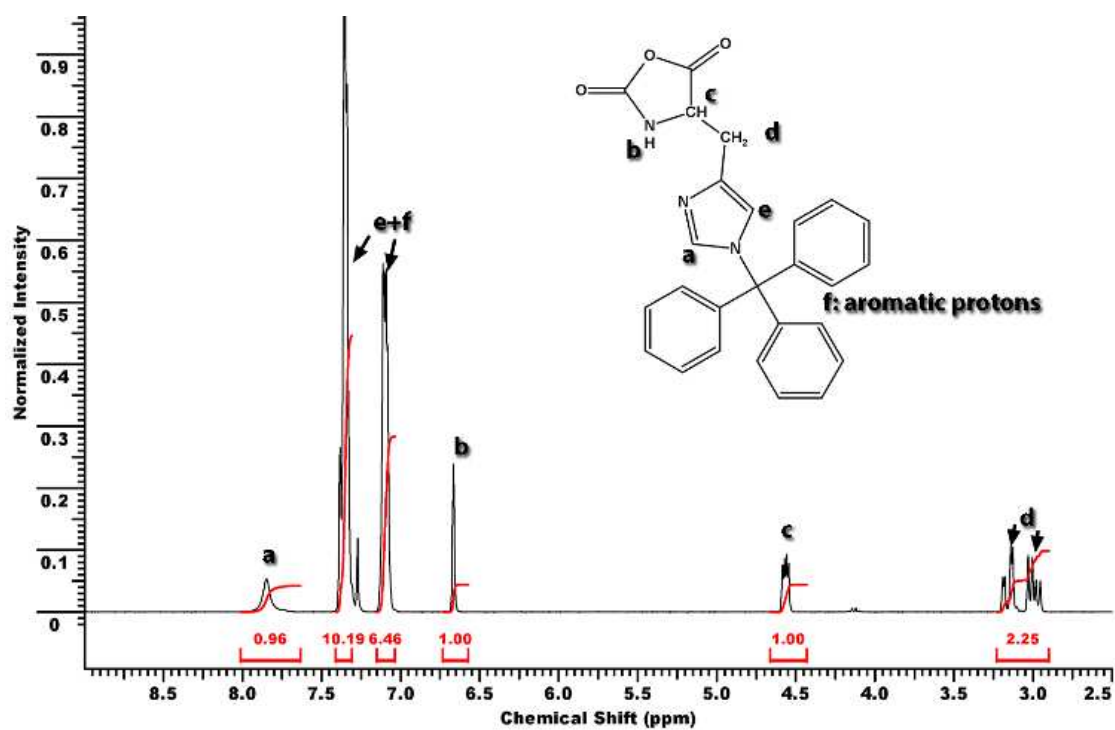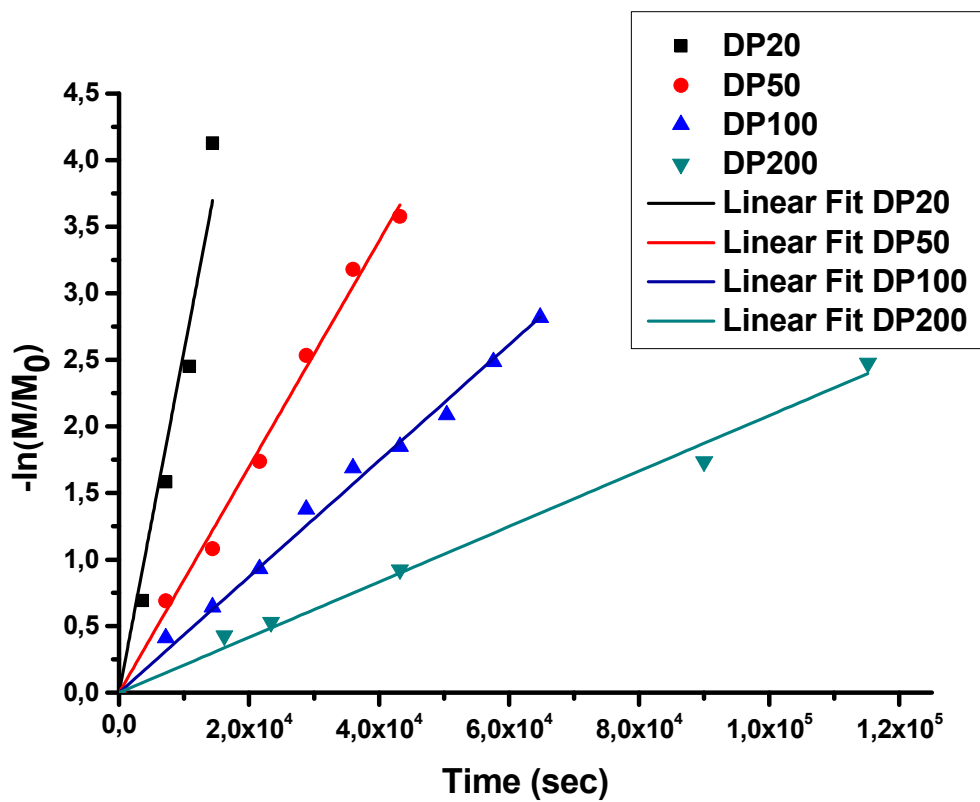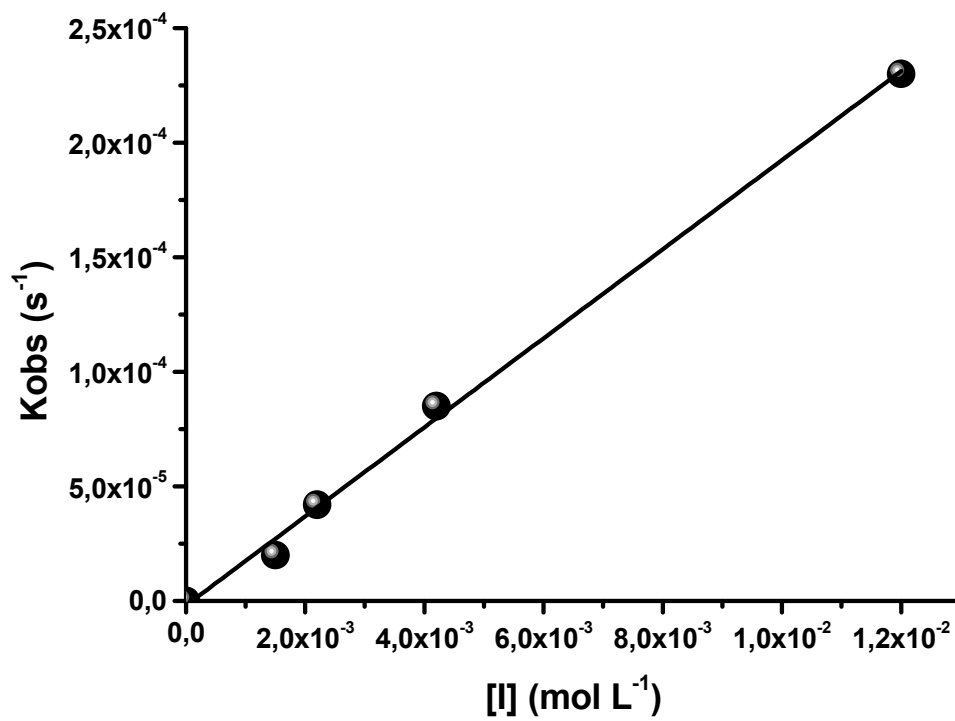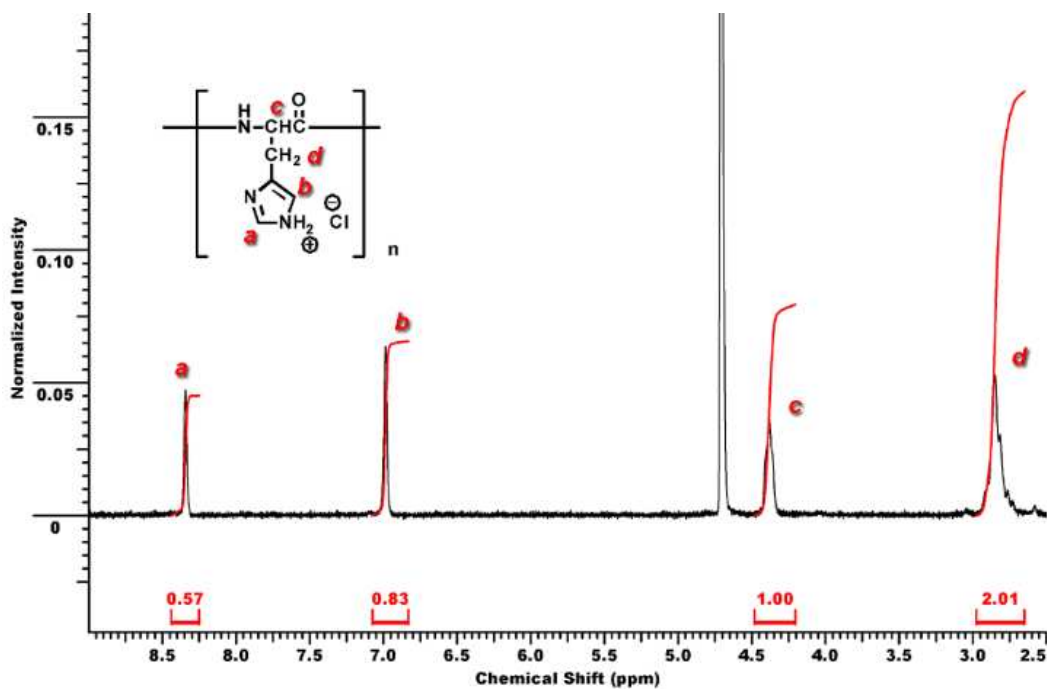
Figure 4

Figure 5

Figure 6
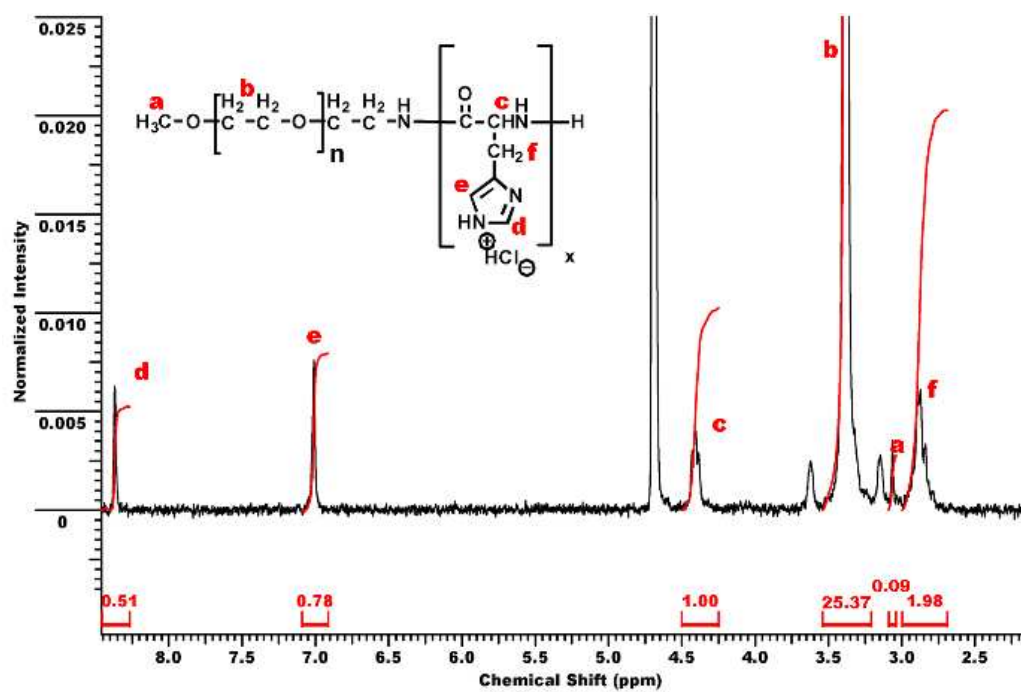
Figure 7
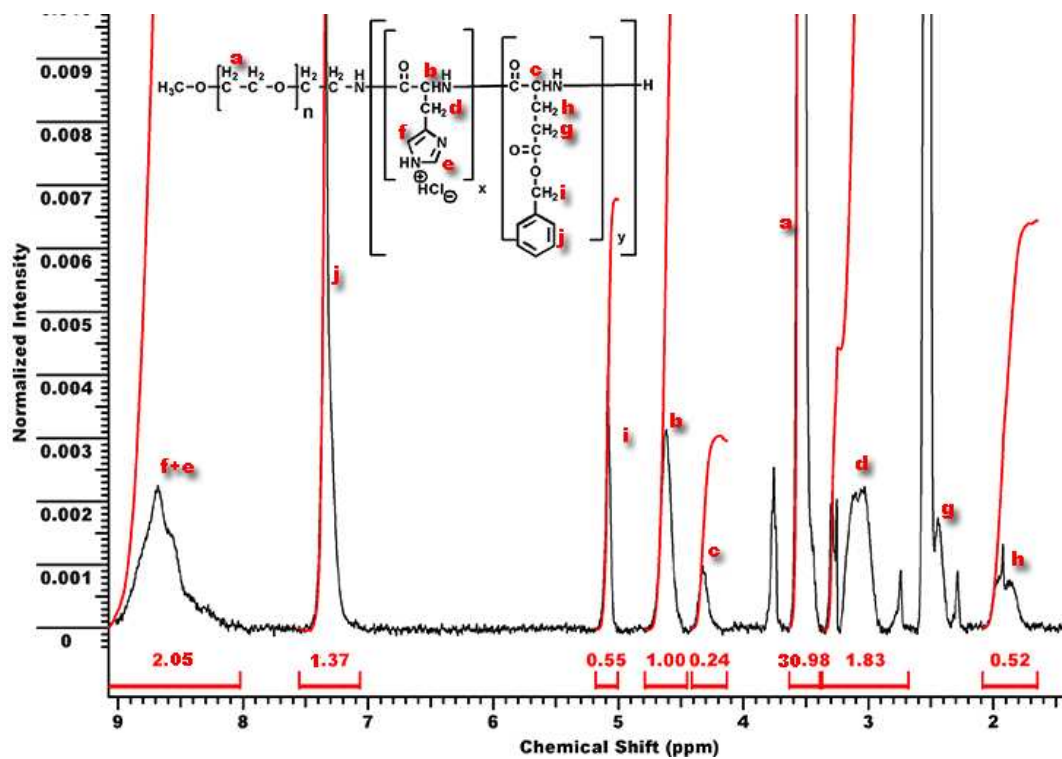
Figure 8
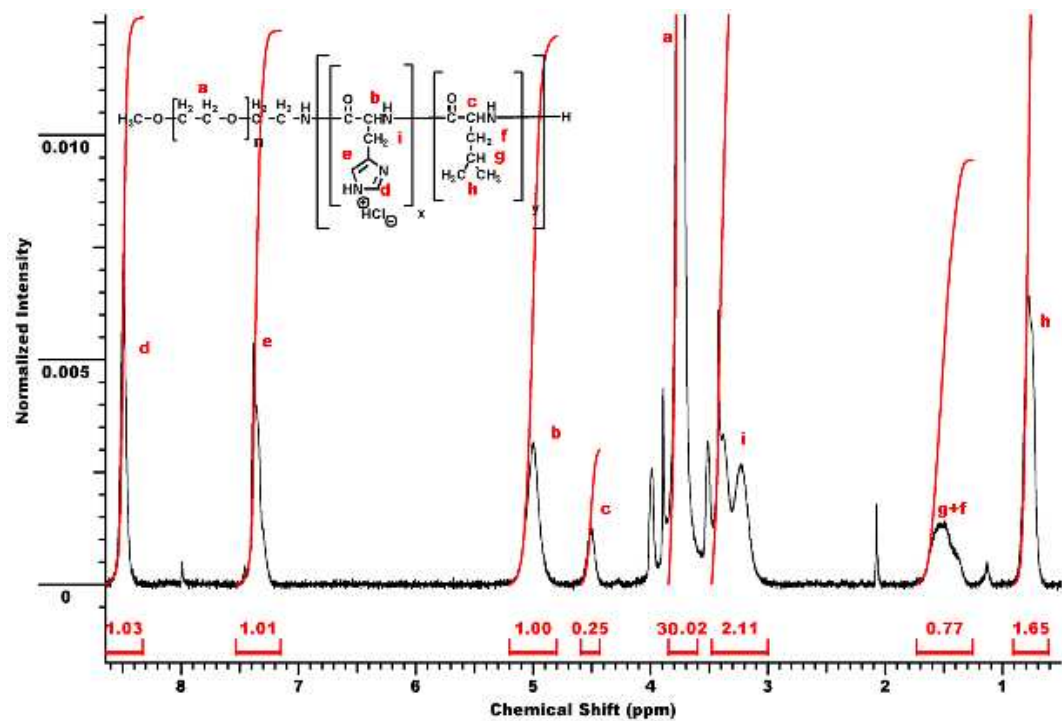
Figure 9
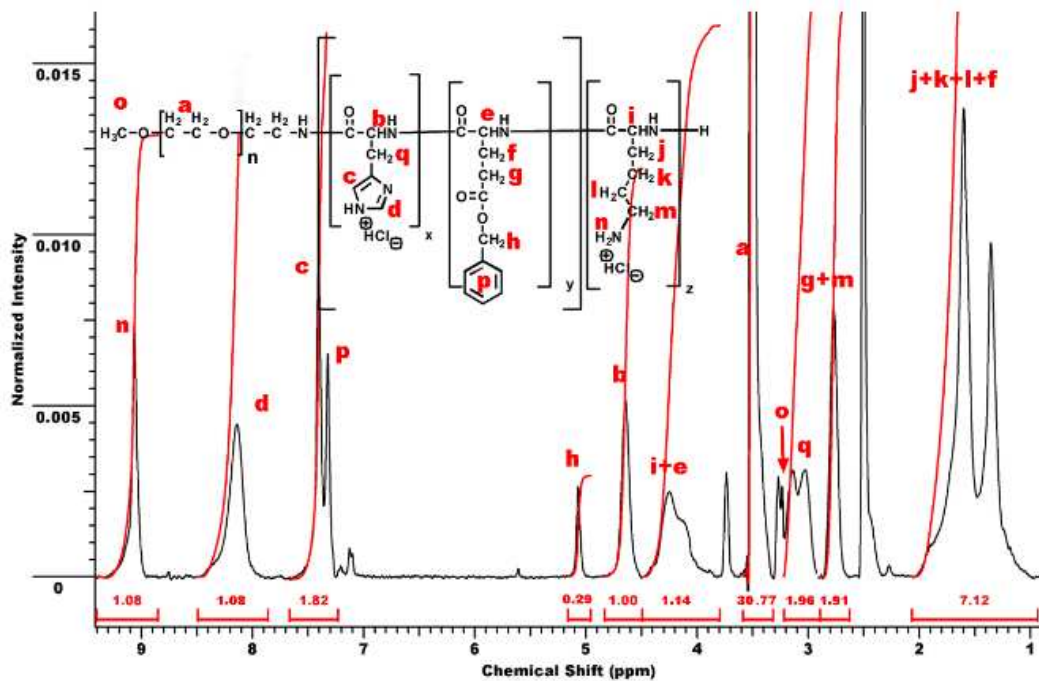
Figure 10
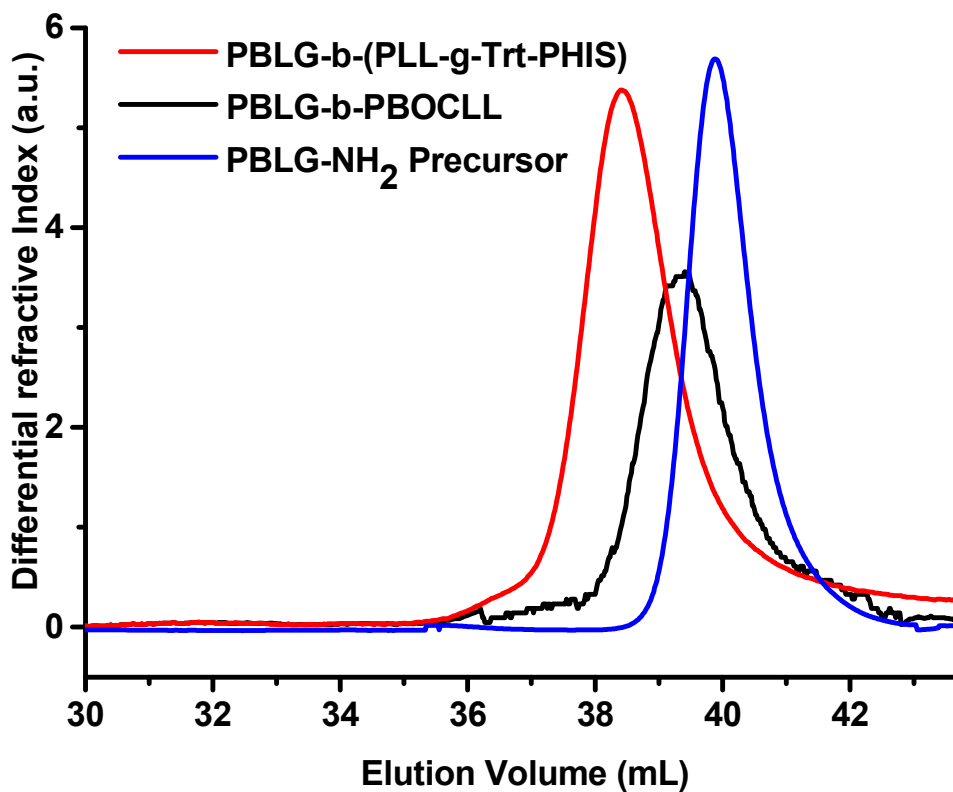
Figure 11
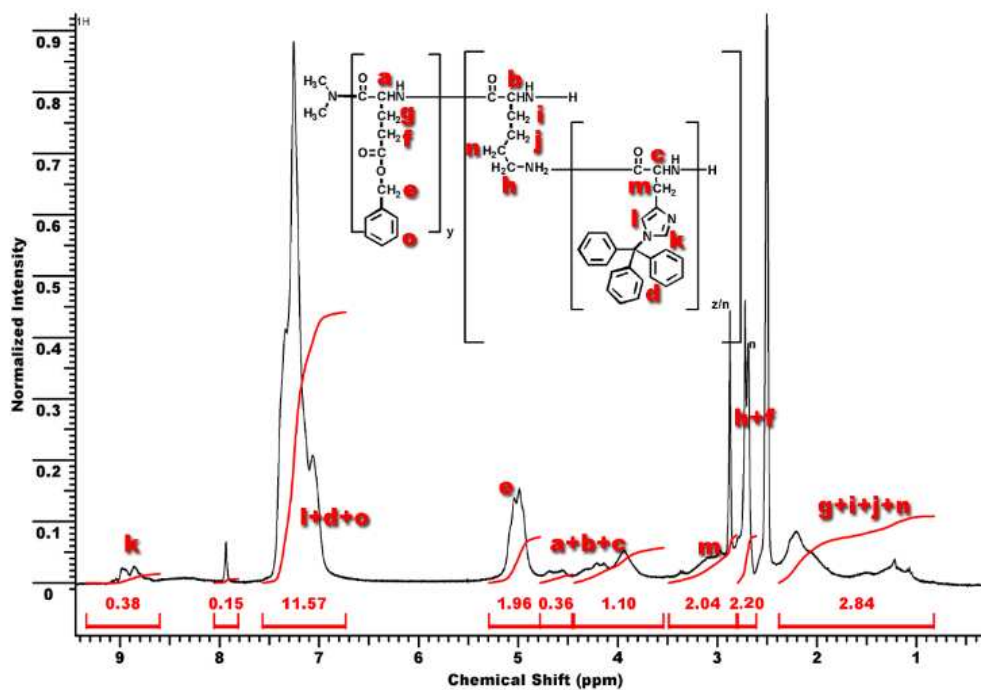
Figure 12
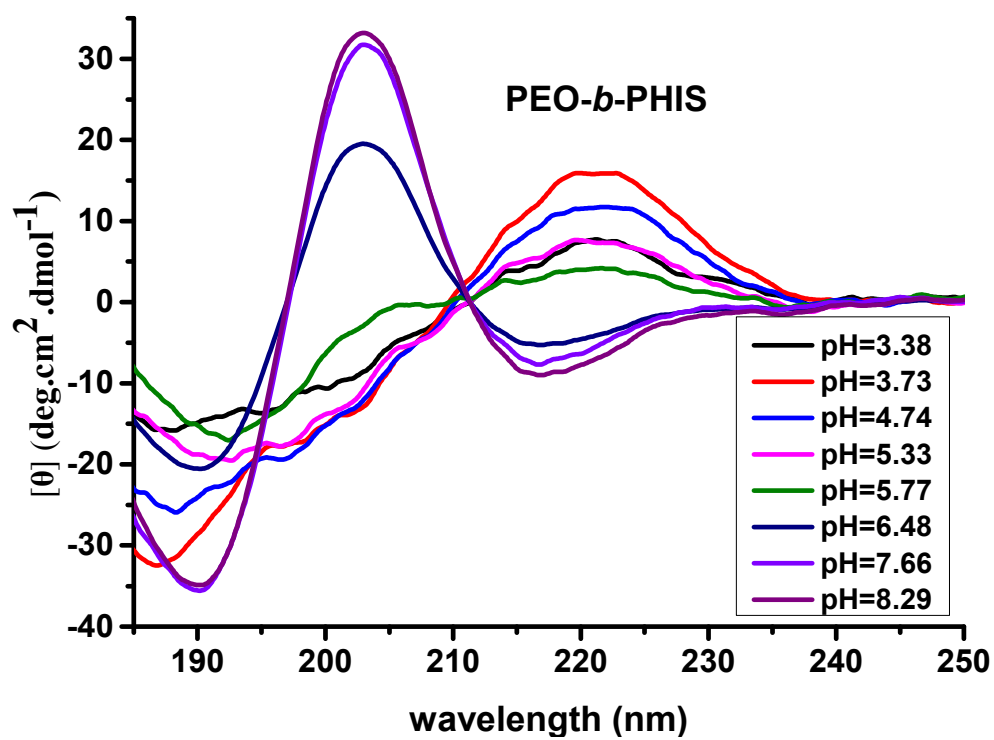
Figure 13
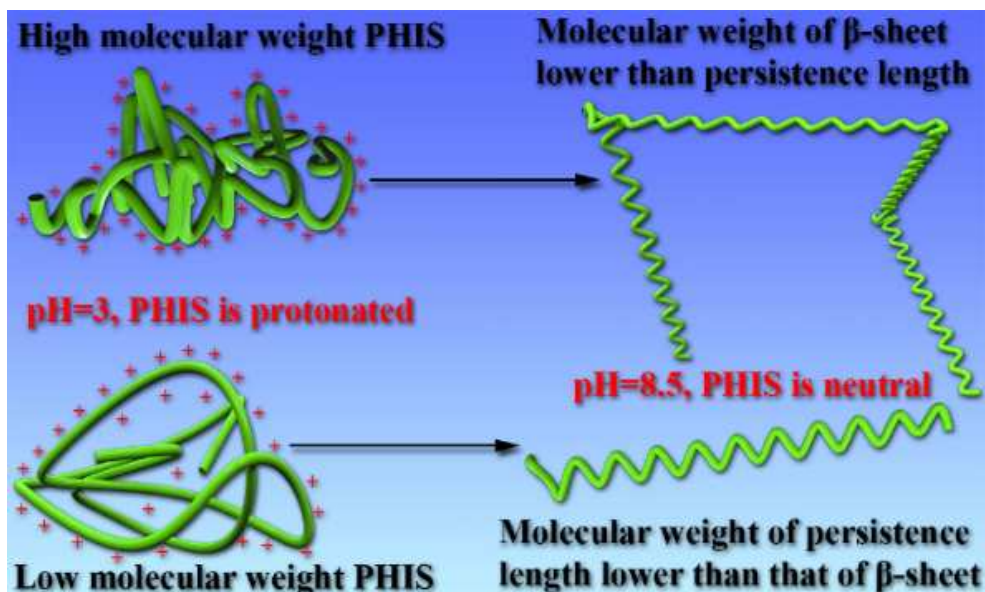
Scheme 10
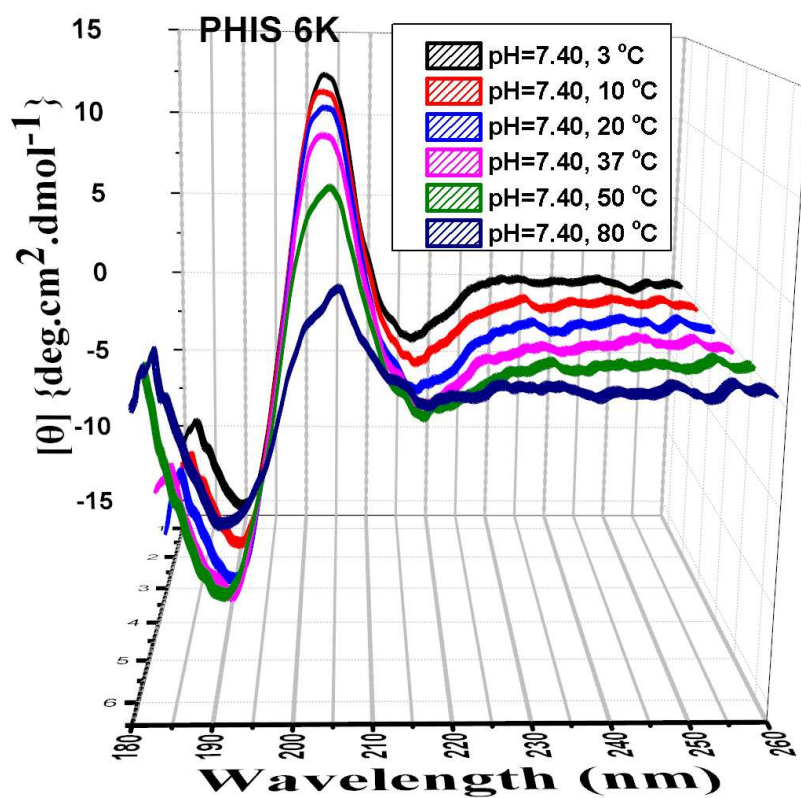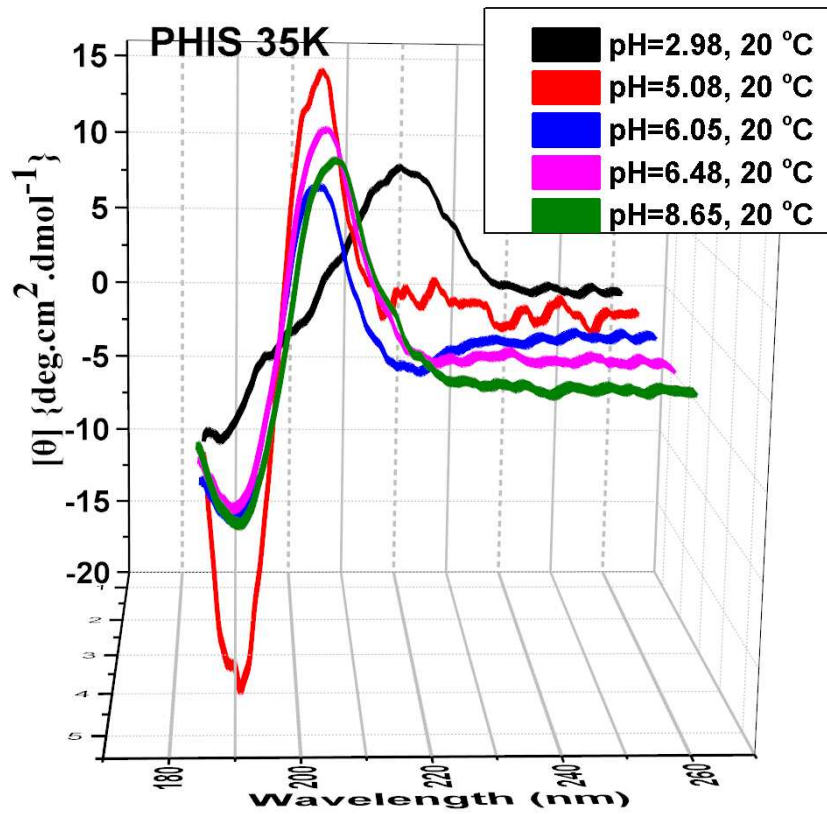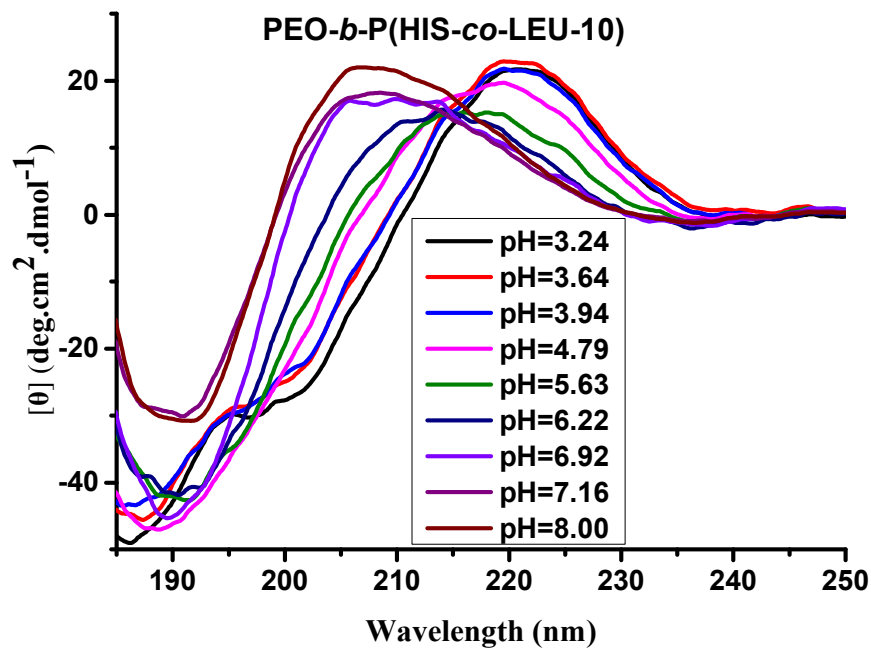
Figure 14

Figure 15

Figure 16
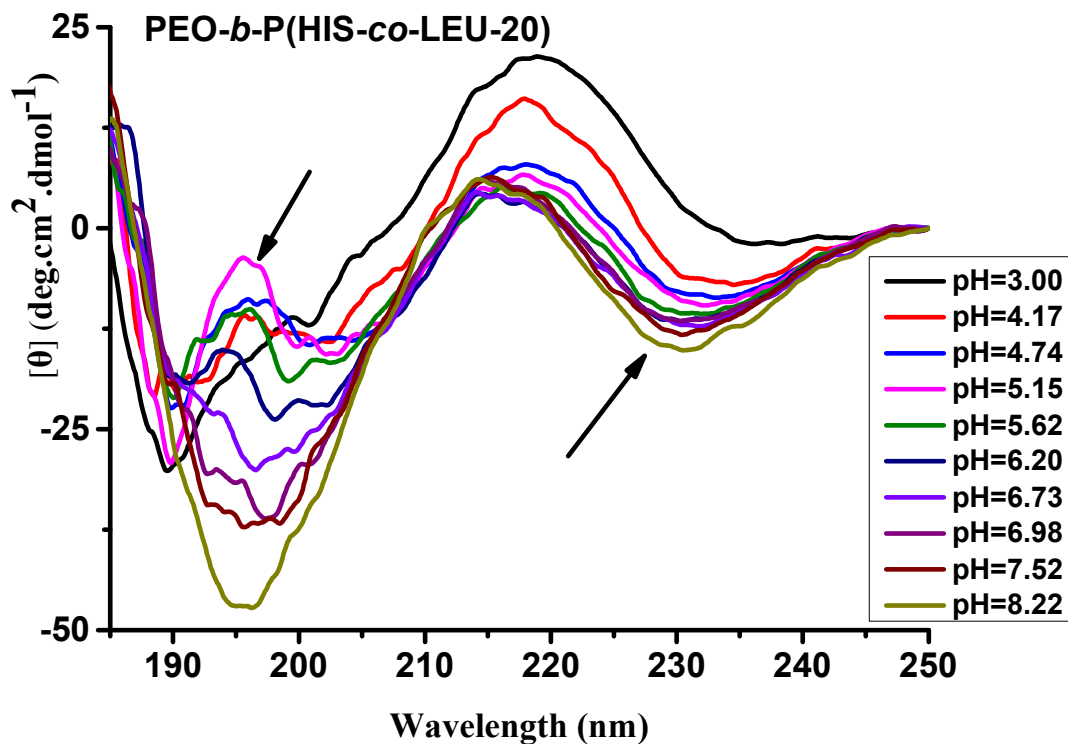
Figure 17
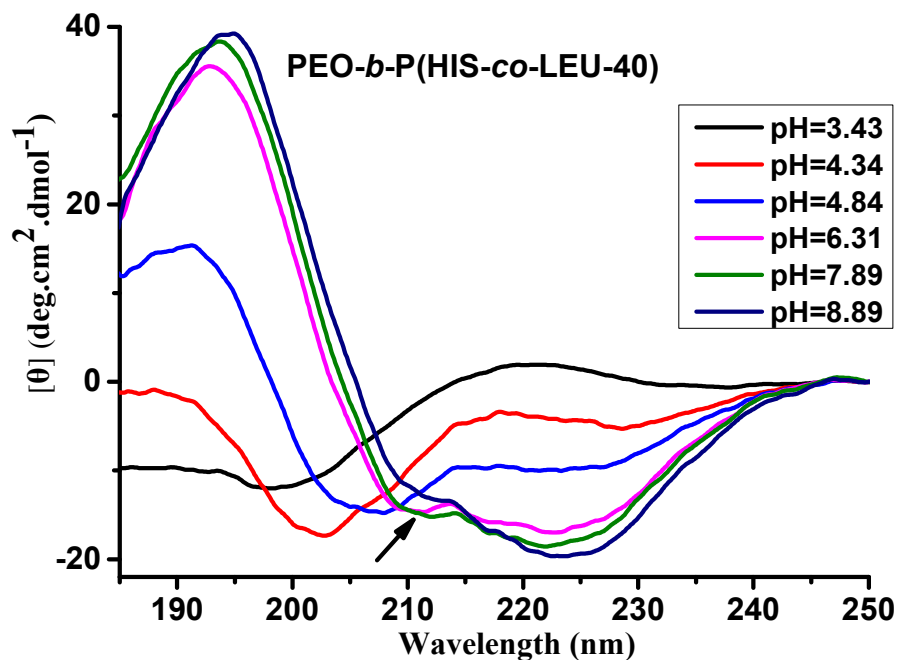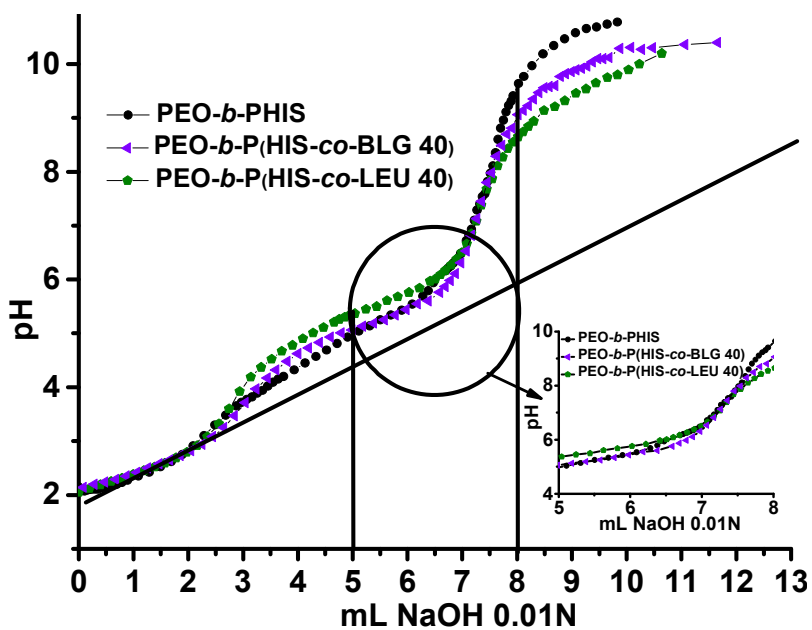

Figure 18

Figure 19
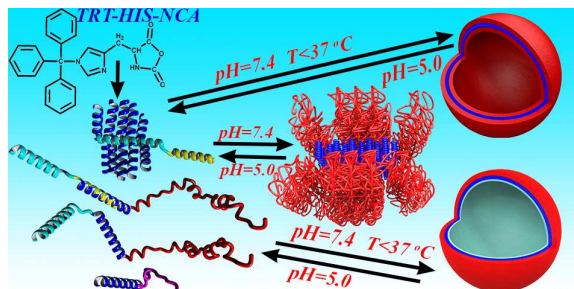

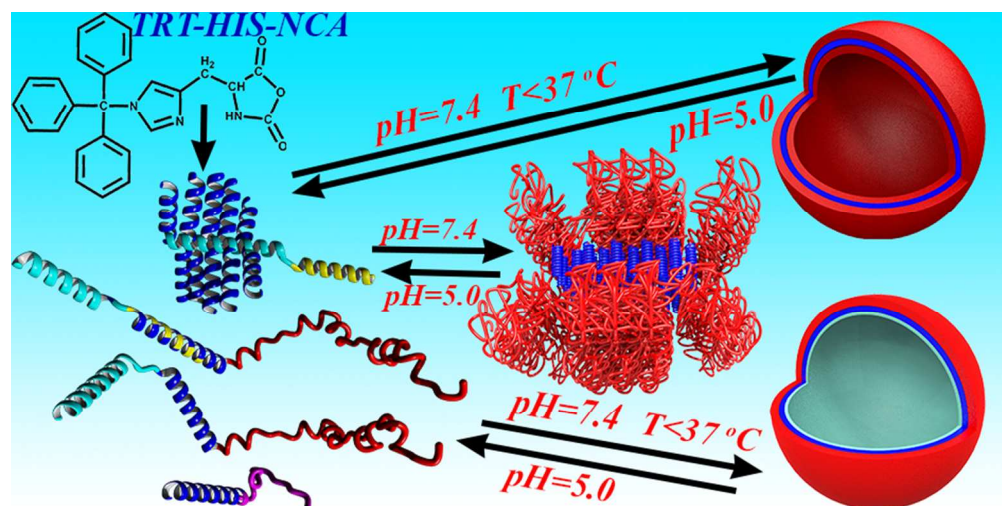**Figure 20**

61
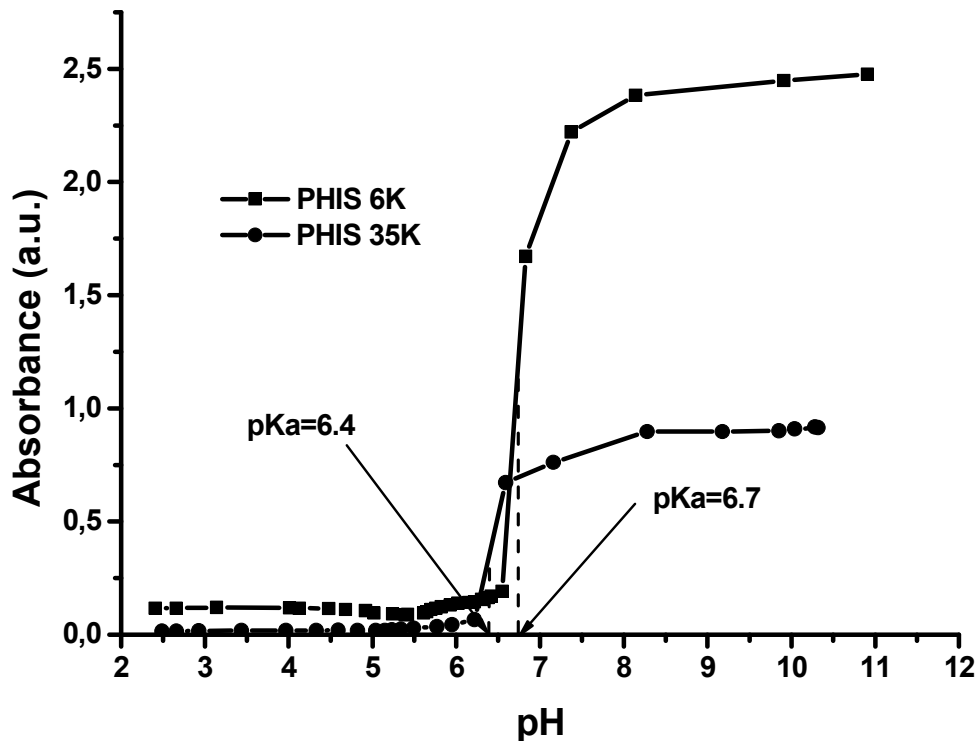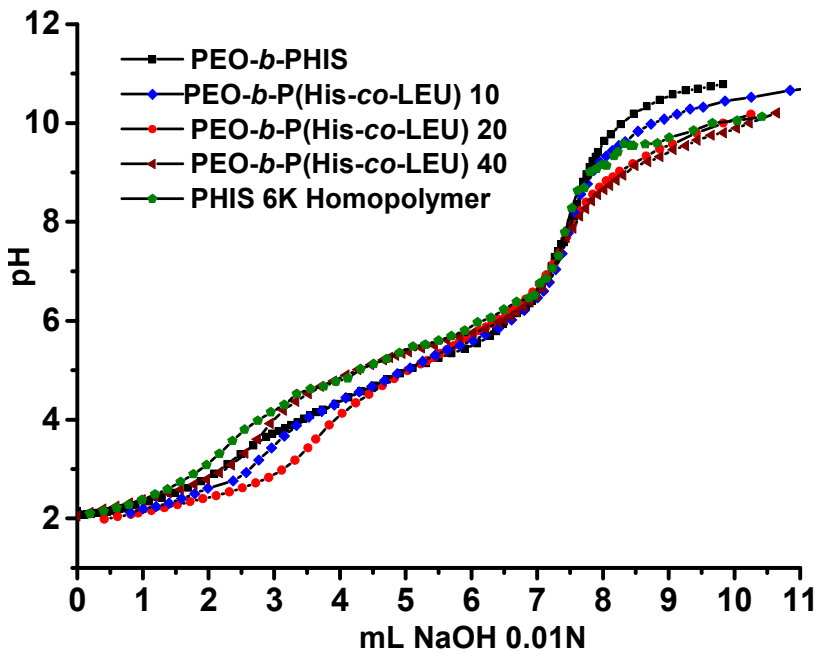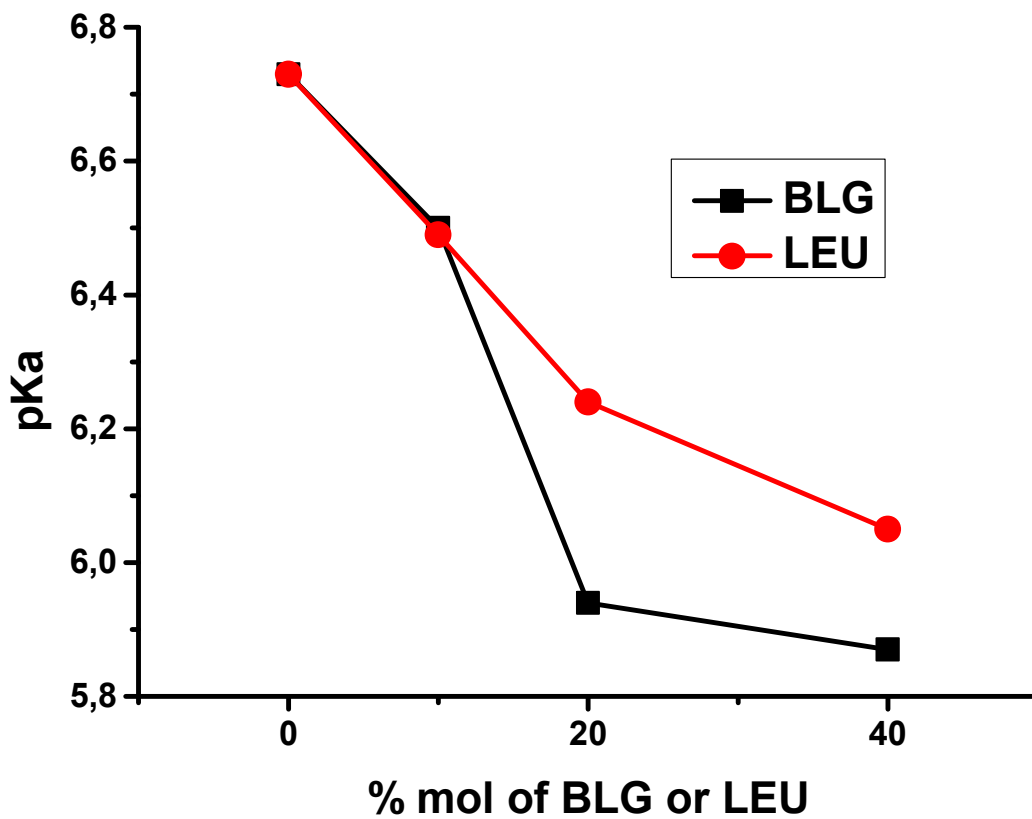
Figure 21

Figure 22

Controlled polymerization of histidine and synthesis of well-defined stimuli responsive polymers. Elucidation of the structure-aggregation relationship of this highly multifunctional material

TABLE OF CONTENTS ENTRY

GRAPHICAL ABSTRACT

Poly(L-histidine) (PHIS) is a highly multifunctional material. Its sol-gel transition within physiological pH renders it unique among all amino acids. However, so far there is no work to present the synthesis of well-defined polymers through a living polymerization process. Therefore its properties has not been studied systematically. We synthesized a novel monomer that leaded to the synthesis of model polymers containing PHIS in a variety of macromolecular architectures. Kinetic studies revealed a living polymerization. Their properties were examined concerning the secondary structure and the degree of protonation which is related to the aggregation behavior of PHIS as a function of pH and temperature. For the first time it was found that besides its pH stimuli responsiveness it respond also to temperature and both stimuli depend on the molecular weight. Hydrophobic amino acids randomly distributed along PHIS chain can lower its pKa. This study give the ability to fine tune the pH where PHIS will be protonated and therefore its aggregates will be ruptured. This is a critical on drug and gene delivery applications.

Controlled polymerization of histidine and synthesis of well-defined stimuli responsive polymers. Elucidation of the structure-aggregation relationship of this highly multifunctional material
80x39mm (300 x 300 DPI)